COMPUTER RESEARCH AND MODELING
2024 VOL. 15 NO. 6 P. e1573–e1600
DOI: 10.20537/2076-7633-2024-15-6-1573-1600

Ки&М

MODELS IN PHYSICS AND TECHNOLOGY

UDC: 519.6 + 539.182

The problem of choosing solutions in the classical format of the description of a molecular system

K. E. Plokhotnikov[1,2]

[1]M. V. Lomonosov Moscow State University,
1/2 Leninskie Gory, Moscow, 119991, Russia
[2]Financial University under the Government of the Russian Federation,
49/2 Leningradsky prospekt, Moscow, 125167, Russia

E-mail: psygma@yandex.ru

Received 24.07.2023, after completion — 11.09.2023.
Accepted for publication 02.10.2023.

The numerical methods developed by the author recently for calculating the molecular system based on the direct solution of the Schrodinger equation by the Monte Carlo method have shown a huge uncertainty in the choice of solutions. On the one hand, it turned out to be possible to build many new solutions; on the other hand, the problem of their connection with reality has become sharply aggravated. In *ab initio* quantum mechanical calculations, the problem of choosing solutions is not so acute after the transition to the classical format of describing a molecular system in terms of potential energy, the method of molecular dynamics, etc. In this paper, we investigate the problem of choosing solutions in the classical format of describing a molecular system without taking into account quantum mechanical prerequisites. As it turned out, the problem of choosing solutions in the classical format of describing a molecular system is reduced to a specific marking of the configuration space in the form of a set of stationary points and reconstruction of the corresponding potential energy function. In this formulation, the solution of the choice problem is reduced to two possible physical and mathematical problems: to find all its stationary points for a given potential energy function (the direct problem of the choice problem), to reconstruct the potential energy function for a given set of stationary points (the inverse problem of the choice problem). In this paper, using a computational experiment, the direct problem of the choice problem is discussed using the example of a description of a monoatomic cluster. The number and shape of the locally equilibrium (saddle) configurations of the binary potential are numerically estimated. An appropriate measure is introduced to distinguish configurations in space. The format of constructing the entire chain of multiparticle contributions to the potential energy function is proposed: binary, three-particle, etc., multiparticle potential of maximum partiality. An infinite number of locally equilibrium (saddle) configurations for the maximum multiparticle potential is discussed and illustrated. A method of variation of the number of stationary points by combining multiparticle contributions to the potential energy function is proposed. The results of the work listed above are aimed at reducing the huge arbitrariness of the choice of the form of potential that is currently taking place. Reducing the arbitrariness of choice is expressed in the fact that the available knowledge about the set of a very specific set of stationary points is consistent with the corresponding form of the potential energy function.

Keywords: problem of choice of solutions, space marking, monatomic cluster, computational experiment, gradient descent, potential energy function, binary and multiparticle potentials

Citation: *Computer Research and Modeling*, 2024, vol. 15, no. 6, pp. e1573–e1600.

КОМПЬЮТЕРНЫЕ ИССЛЕДОВАНИЯ
И МОДЕЛИРОВАНИЕ 2024 Т. 15 № 6 С. e1573–e1600
DOI: 10.20537/2076-7633-2024-15-6-1573-1600

Ки&М

МОДЕЛИ В ФИЗИКЕ И ТЕХНОЛОГИИ

УДК: 519.6 + 539.182

Проблема выбора решений при классическом формате описания молекулярной системы

К. Э. Плохотников[1,2]

[1]МГУ им. М. В. Ломоносова,
Россия, 119991, ГСП-1, г. Москва, Ленинские горы, д. 1, стр. 2
[2]Финансовый университет при Правительстве РФ,
Россия, 125167, г. Москва, проспект Ленинградский, д. 49, стр. 2

E-mail: psygma@yandex.ru

Получено 24.07.2023, после доработки — 11.09.2023.
Принято к публикации 02.10.2023.

Разработанные автором недавно численные методики расчета молекулярной системы на базе прямого решения уравнения Шрёдингера методом Монте-Карло показали огромную неопределенность в выборе решений. С одной стороны, оказалось возможным построить множество новых решений, с другой стороны, резко обострилась проблема их связывания с реальностью. В квантовомеханических расчетах *ab initio* проблема выбора решений стоит не так остро после перехода к классическому формату описания молекулярной системы в терминах потенциальной энергии, метода молекулярной динамики и пр. В данной работе исследуется проблема выбора решений при классическом формате описания молекулярной системы без учета квантовомеханических предпосылок. Как оказалось, проблема выбора решений при классическом формате описания молекулярной системы сводится к конкретной разметке конфигурационного пространства в виде набора стационарных точек и реконструкции соответствующей функции потенциальной энергии. В такой постановке решение проблемы выбора сводится к двум возможным физико-математическим задачам: по заданной функции потенциальной энергии найти все ее стационарные точки (прямая задача проблемы выбора), по заданному набору стационарных точек реконструировать функцию потенциальной энергии (обратная задача проблемы выбора). В работе с помощью вычислительного эксперимента обсуждается прямая задача проблемы выбора на примере описания моноатомного кластера. Численно оцениваются число и форма локально равновесных (седловых) конфигураций бинарного потенциала. Вводится соответствующая мера по различению конфигураций в пространстве. Предлагается формат построения всей цепочки многочастичных вкладов в функцию потенциальной энергии: бинарный, трехчастичный и т. д., многочастичный потенциал максимальной частичности. Обсуждается и иллюстрируется бесконечное количество локально равновесных (седловых) конфигураций для максимально многочастичного потенциала. Предлагается методика вариации числа стационарных точек путем комбинирования многочастичных вкладов в функцию потенциальной энергии. Перечисленные выше результаты работы направлены на то, чтобы уменьшить тот огромный произвол выбора формы потенциала, который имеет место в настоящее время. Уменьшение произвола выбора выражается в том, что имеющиеся знания о вполне конкретном наборе стационарных точек согласуются с соответствующей формой функции потенциальной энергии.

Ключевые слова: проблема выбора решений, разметка пространства, моноатомный кластер, вычислительный эксперимент, градиентный спуск, функция потенциальной энергии, бинарный и многочастичный потенциалы

1. Introduction

In earlier works by the present author [Плохотников, 2019; Plokhotnikov, 2021], a numerical method for solving the Schrödinger equation to describe an arbitrary quantum system is presented. The described method is developed at the intersection of finite difference and Monte Carlo approaches. This method has proved to be very effective in terms of low machine time costs provided that the average positions of the particle nuclei of the quantum system are known. To determine the latter, an-other computational technique was developed [Плохотников, 2020], which is based on the virial theorem and reduction to a multiple solution of the equation "the potential energy of a quantum system is equal to two dissociation energies" with subsequent averaging of the found positions.

Further development of this computational approach is associated with the quantum mechanical description of water clusters [Плохотников, 2022b; Plokhotnikov, 2022]. From the description of clusters of water molecules, it became clear how to lead the electronic and ionic components of a quantum system in space to obtain the desired quantum mechanical solution. Accordingly, there turned out to be an infinite number of solutions describing an arbitrary quantum system to permit the construction of a statistical generator of solutions to the Schrödinger equation [Плохотников, 2022a; Plokhotnikov, 2023]. The problem of choosing a solution from an infinite number, which is well known, e. g., in the theory of quantum measurements [Менский, 1983; Броер, Петруччионе, 2010; Schlosshauer, 2019; Zurek, 2022], becomes especially acute after constructing a statistical generator of solutions to the Schrödinger equation.

In general, all the so-called *ab initio* calculations [Хартри, 1960; Kohn, 1999; Kim et al., 2018] in quantum mechanics proceed from some (explicitly or implicitly accepted) *a priori* spatial markup of a quantum system. Such a specified spatial markup can be provided by constructing the corresponding potential energy function [Car, Parrinello, 1985; Marx, Hutter, 2009; Kühne et al., 2020], which is expressed in terms of the positions of the particle nuclei of the quantum system. In the latter case, the so-called Born – Oppenheimer approximation is used.

Since the topic discussed in the article arose on the way to solving the Schrödinger equation, we present the main results with minimal use of the appropriate formulas, focusing on appropriate interpretations and conclusions.

The presented task was to numerically solve the Schrödinger equation describing an arbitrary quantum system using the Monte Carlo method. Let us write down the Schrödinger equation describing in dimensionless form the dynamics of a quantum system consisting of n particles, i. e.,

$$i\psi_t = -\frac{1}{2}\sum_{j=1}^{n}\mu_j\Delta_j\psi + U\psi,$$

where $\psi_t = \frac{\partial\psi}{\partial t}$, $\Delta_j\psi = \frac{\partial^2\psi}{\partial x_j^2} + \frac{\partial^2\psi}{\partial y_j^2} + \frac{\partial^2\psi}{\partial z_j^2}$, $U = U(\mathbf{r}_1, \ldots, \mathbf{r}_n) = \sum\limits_{1=j<k=n}\frac{q_iq_j}{|\mathbf{r}_j-\mathbf{r}_k|}$ — Coulomb potential energy, $i^2 = -1$, $\mu_j = \frac{m_e}{m_j}$ — the ratio of the mass of an electron m_e to the mass of a quantum particle m_j, q_j — particle charges expressed in units of electron charge, $\psi = \psi(t, \mathbf{r}_1, \ldots, \mathbf{r}_n)$ — a wave function describing a quantum system, t — time, $\mathbf{r}_1, \ldots, \mathbf{r}_n$ — the spatial positions of each of the quantum particles in three-dimensional space.

In the numerical algorithm for solving the Schrödinger equation presented below, described in the works of the author [Плохотников, 2019; Plokhotnikov, 2021], the molecular system is either split into N copies or each quantum particle (both the nuclei of elements and electrons) is represented as N subparticles. Let the dissociation energy of a quantum system be E_Σ, then the algorithm for solving the Schrödinger equation is reduced to the following computational steps.

1. Let us introduce N radius vectors $r_i = (\mathbf{r}_{1,i}, \ldots, \mathbf{r}_{n,i})$, $i = 1, \ldots, N$ in a space of dimension $3n$ according to point 4 of this algorithm.

2. Let us make up a matrix $Q = \frac{1}{2}\varepsilon N e_N - \frac{1}{2}\varepsilon o_N + \mathrm{diag}(U_i)$, where $\varepsilon = -\frac{2E_\Sigma}{N}$ is a non-negative parameter that ensures the fulfillment of the conditions of the virial theorem in relation to the molecular system, e_N is a single matrix in size $N \times N$, o_N is a special matrix in size $N \times N$, all elements of which are units, $\mathrm{diag}(U_i)$ is a diagonal matrix in size $N \times N$, on the diagonals of which are the values of the potential energy of the molecule at points r_i, $i = 1, \ldots, N$. The potential energy of the system is calculated using the formula: $U_i = \sum\limits_{1=j<k=n} \frac{q_i q_j}{|\mathbf{r}_{j,i} - \mathbf{r}_{k,i}|}$.

3. Find the eigenvalues $\Omega_1, \ldots, \Omega_N$ and eigenvectors $c_1, \ldots, c_N$ of the matrix Q. Let us choose among the set of eigenvalues the one $\Omega_\alpha \cong E_\Sigma$, that is closest to the total energy of the molecule, i. e. $\alpha = \arg\min\limits_{1 \leqslant i \leqslant N} |\Omega_i - E_\Sigma|$. Assuming that the eigenvectors are normalized by one, we will find the localization $\mathbf{R}_{k,\alpha}$, $k = 1, \ldots, n$ of the positions of the quantum particles included in the quantum system: $\mathbf{R}_{k,\alpha} = \sum\limits_{i=1}^{N} c_{\alpha,i}^2 \mathbf{r}_{k,i}$.

4. Repeat the procedure in part 1–3 M times, assuming that the radius vectors $r_i = (\mathbf{r}_{1,i}, \ldots, \mathbf{r}_{n,i})$, $i = 1, \ldots, N$ are selected each time according to the scheme of the form: $\mathbf{r}_{k,i} = \mathbf{a}_k + \sigma 2L\sqrt{\mu_k}\boldsymbol{\eta}_{k,i}$, $k = 1, \ldots, n$; $i = 1, \ldots, N$, where $\mathbf{a}_k$, $k = 1, \ldots, n$ — the so-called scattering centers (middle positions) of quantum particles; σ — some non-negative fitting coefficient; L — typical task size; $\boldsymbol{\eta}_{k,i}$, $k = 1, \ldots, n$, $i = 1, \ldots, N$ — vectors of independent random variables whose coordinates have zero mathematical expectation and variance of the order of one.

The numerical algorithm presented above for solving the Schrödinger equation is aimed at searching for pure states of a quantum system. Taking into account the central limit theorem of probability theory, this algorithm was found to become more and more accurate with an increase in the number of particles in a quantum system; with the number of quantum particles exceeding several dozen, its accuracy is quite satisfactory. The spatial construction of scattering clouds of all particles of the quantum system at the output of using this algorithm is considered as a solution to the Schrödinger equation.

Using the example of modeling water clusters using the specified numerical method, the choice of input parameters comprising the average positions of particles $\mathbf{a}_1, \ldots, \mathbf{a}_n$ turned out to be associated with the statistical agreement of the positions of positively charged particle nuclei and electrons. This coordination is referred to as a procedure for leading together the nuclei of particles and electrons despite the huge arbitrariness in choosing the positions of the nuclei of particles. As a result, a so-called statistical generator of solutions to the Schrödinger equation was constructed [Плохотников, 2022a; Plokhotnikov, 2023]. Although there turned out to be infinitely many such solutions, this is typical for any partial differential equation; the Schrödinger equation is no exception in this regard. Thus, there are infinitely many solutions; moreover, they are not subordinated to each other, as is the case with the classical format of describing a molecular system, e. g., using the molecular dynamics method.

From this stage, the problem of choosing solutions arose. On the one hand, there are infinitely many solutions, and they are equally possible, as indicated by the statistical solution generator. On the other hand, there is not an infinite number of solutions in the face of a set of local minima of the potential energy function, as in the method of molecular dynamics. The question then arises: is not the method of molecular dynamics — and, accordingly, the classical format of the description of a molecular system — a way, if not to solve, then at least to mitigate the problem of choosing solutions? It was this circumstance that gave rise to the present work.

Let us return now to the material under consideration. For simplicity, consider a monoatomic quantum system consisting of N identical atoms. According to the numerical approach mentioned above, it follows that the average positions, $\mathbf{r}_1 = (x_1, y_1, z_1), \ldots, \mathbf{r}_N = (x_N, y_N, z_N)$ of the particle nuclei can be arbitrarily moved; following a special procedure for spatial bring of electrons with particle nuclei, new acceptable solutions can be obtained by the Schrödinger equation. In fact, from the point of view of the Schrödinger equation, there is no spatial markup in the quantum system. This arises, for example, when switching to the description of a quantum system in the language of molecular dynamics [Stillinger, Weber, 1984; Товбин, 1996; Frenkel, Smit, 2002], where, as is known, the central role is played by the function of potential energy $U = U(\mathbf{r}_1, \ldots, \mathbf{r}_N)$. It is the latter, comprising a function of $3N$ variables through its stationary points, that provides the appropriate markup for both the configuration space of dimensions $3N$ and the three-dimensional space in which the quantum system under study is placed.

In contradistinction with the works [Wales, 2002; Wales, 2009; Röder, Wales, 2022], in which the reaction rates are calculated taking into account the layout of the configuration space, the molecular system is considered in the present work from the point of view of statistical physics as a canonical ensemble at zero temperature. Modern digital designers of molecular systems [Amber Project, 2023; HyperChem, 2009] concentrate the classical format for describing a complex system. In the above-mentioned and other various constructors, the choice of a class of configurations of a molecular system is determined by the background of the use of one or another classical and (or) quantum methods of description, while in all cases the inclusion of certain atoms or molecular subsystems in the desired design does not imply their radical transformation.

First, let us assume that there are a finite number of stationary points N_{stp} of the potential energy function U (up to shifts, rotations and permutations of particles) and they are isolated from each other. As is known, stationary points are those points $o_1, \ldots, o_{N_{stp}}$ in the configuration space of dimension $3N$ in which the gradient of the potential energy function takes on a zero value, i. e.

$$U_{x_i}(o_l) = \frac{\partial U(o_l)}{\partial x_i} = 0, \quad U_{y_i}(o_l) = \frac{\partial U(o_l)}{\partial y_i} = 0, \quad U_{z_i}(o_l) = \frac{\partial U(o_l)}{\partial z_i} = 0, \tag{1}$$

where $l = 1, \ldots, N_{stp}$, $i = 1, \ldots, N$.

A set of stationary points $o_1, \ldots, o_{N_{stp}}$ is insufficient for the desired marking of the configuration space and removing the problem of choosing a solution. Since we want to obtain information about the nature of each of the stationary points, it will be necessary to study the matrix of the second derivatives H of the potential energy function in order to count the number of positive p_l, $l = 1, \ldots, N_{stp}$ and negative m_l, $l = 1, \ldots, N_{stp}$ eigenvalues. At the same time $p_l + m_l \leqslant \mathrm{rank}(H)$, where $\mathrm{rank}(H)$ is the rank of the Hesse matrix of potential energy. Since the potential energy function is generally invariant with respect to arbitrary shifts and rotations in the three-dimensional space of a quantum system as a whole, its rank does not exceed the value $3N - 6$. Thus, the inequality is true for each of the stationary points: $p_l + m_l \leqslant 3N - 6$, $l = 1, \ldots, N_{stp}$. Since the values p_l, m_l are non-negative, insofar p_l, $m_l = 0, 1, \ldots, 3N - 6$ for any stationary point, i. e., when $l = 1, \ldots, N_{stp}$.

All stationary points are divided into three categories: 1) local minima in which $p_l > 0$, $m_l = 0$; 2) saddle points in which $p_l > 0$, $m_l > 0$; 3) local maxima in which $p_l = 0$, $m_l > 0$. Taking into account the mentioned terminology, it is clear that an arbitrary image point in the configuration space, from the point of view of classical forces determined by the anti-gradient of potential energy, moves from one stationary point to another. Under certain conditions, this movement ends with the localization of the image point in one of the local minima. If we now assume that the energy from the molecular system not only goes away during the transition to a local minimum, but also enters, then the image point can be considered as wandering along stationary points.

As a result, the classical method of removing quantum uncertainty in choosing a solution to the Schrödinger equation is reduced to calculating a set of stationary points $o_1, \ldots, o_{N_{stp}}$ with given characteristics in the face of the number of positive p_l, $l = 1, \ldots, N_{stp}$ and negative m_l, $l = 1, \ldots, N_{stp}$ eigenvalues of the Hesse matrix of potential energy. The task of identifying the markup is typically solved with a given potential energy function. However, the inverse problem of reconstructing potential energy according to a given markup looks much more complicated and uncertain. According to the results of the computational experiment presented in the paper, the number of stationary points can be infinite and even uncountable under certain conditions.

Thus, two physical and mathematical problems can be formulated. The first, direct problem of choosing solutions: uses a given potential energy function, to find all stationary points (sets of stationary points), i. e., determine the marking up of the configuration space. The second, inverse problem of choosing solutions involves a reconstruction of the potential energy function according to a given set of stationary points (a set of stationary points), i. e., according to a given marking up of the configuration space. In the present paper, the solution of a direct problem is discussed using the example of a description of a monoatomic cluster.

2. The spectrum of multiparticle forms of potential representation

Let us construct a spectrum of multiparticle potentials, starting with binary or two-particle, U_2, three-particle, U_3, etc. up to the maximum particle potential, U_N. We will construct a set of multiparticle potentials $U_\alpha = U_\alpha(\mathbf{r}_1, \ldots, \mathbf{r}_N)$, $\alpha = 2, \ldots, N$ by induction.

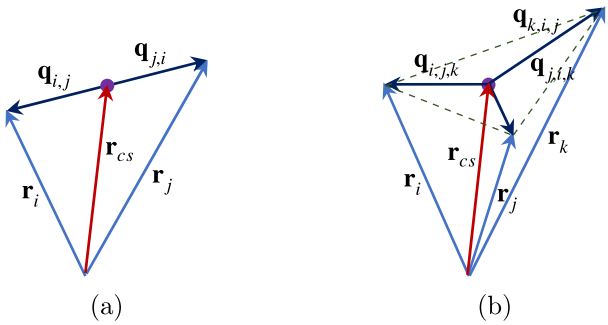

Figure 1. Radius vector positioning schemes for binary (a) and three-particle (b) particle interaction schemes in a cluster

Let us define a set of radius vectors $\mathbf{q}_{i,j} = \mathbf{r}_i - \frac{1}{2}(\mathbf{r}_i + \mathbf{r}_j) = \frac{1}{2}\mathbf{r}_{i,j}$, where $\mathbf{r}_{i,j} = \mathbf{r}_i - \mathbf{r}_j$, $i, j = 1, \ldots, N$. By entering the center of symmetry of a pair of identical particles $\mathbf{r}_{cs,i,j} = \frac{1}{2}(\mathbf{r}_i + \mathbf{r}_j)$, the following representation can be written: $\mathbf{r}_i = \mathbf{q}_{i,j} + \mathbf{r}_{cs,i,j}$, $\mathbf{r}_j = \mathbf{q}_{j,i} + \mathbf{r}_{cs,i,j}$. It follows from the latter that a pair of vectors $\mathbf{q}_{i,j}$, $\mathbf{q}_{j,i}$ act as radius vectors directed from the center of symmetry of a pair of particles to the i-th and j-th particles (Fig. 1, *a*). Note that the pairs of particles $\{i, j\}$, $i, j = 1, \ldots, N$ $(i \neq j)$ total $N(N-1)$. We describe the contribution to the potential energy of particle pairs $\{i, j\}$ and $\{j, i\}$ the following expression: $\frac{1}{2}[\varphi_2(|\mathbf{q}_{i,j}|) + \varphi_2(|\mathbf{q}_{j,i}|)]$, where $\varphi_2(\cdot)$ — some as yet undefined function of one variable. Since $\mathbf{q}_{i,j} + \mathbf{q}_{j,i} = \mathbf{0}$, insofar as the contribution of a pair $\{i, j\}$ of particles to the potential energy will be the value $\varphi_2(|\mathbf{q}_{i,j}|)$. As a result, we write down the following representation for the binary potential:

$$U_2 = \frac{1}{2}\sum_{i,j=1\ (i\neq j)}^{N} \varphi_2(|\mathbf{q}_{i,j}|) = \sum_{i<j} \varphi_2(|\mathbf{q}_{i,j}|). \tag{2}$$

Let us build a three-particle potential, U_3. A set of radius vectors $\mathbf{q}_{i,j,k} = \mathbf{r}_i - \frac{1}{3}(\mathbf{r}_i + \mathbf{r}_j + \mathbf{r}_k) = \mathbf{r}_i - \mathbf{r}_{cs,i,j,k} = \frac{1}{3}(2\mathbf{r}_i - \mathbf{r}_j - \mathbf{r}_k)$ is defined, where $\mathbf{r}_{cs,i,j,k}$ — the center of symmetry of the three particles,

$i, j, k = 1, \ldots, N$. It follows from the latter representation that the three vectors $\mathbf{q}_{i,j,k}$, $\mathbf{q}_{j,i,k}$, $\mathbf{q}_{k,i,j}$ act as radius vectors directed from the center of symmetry of the three particles to the i-th, j-th and k-th particles (Fig. 1, *b*). Note that the triples of particles $\{i, j, k\}$, $i, j, k = 1, \ldots, N$ $(i \neq j \neq k \neq i)$ total $N(N-1)(N-2)$. We describe the contribution to the potential energy of all six permutations of triples of particles $\{i, j, k\}$, $\{i, k, j\}$, $\{k, i, j\}$, $\{k, j, i\}$, $\{j, i, k\}$, $\{j, k, i\}$ by the expression:

$$\frac{1}{6}[\varphi_3(|\mathbf{q}_{i,j,k}|) + \varphi_3(|\mathbf{q}_{i,k,j}|) + \varphi_3(|\mathbf{q}_{ij,i,k}|) + \varphi_3(|\mathbf{q}_{ij,k,i}|) + \varphi_3(|\mathbf{q}_{k,i,j}|) + \varphi_3(|\mathbf{q}_{k,j,i}|)],$$

where $\varphi_3(\cdot)$ — as yet undefined function of one variable. Since $\mathbf{q}_{i,j,k} = \mathbf{q}_{i,k,j}$, $\mathbf{q}_{j,i,k} = \mathbf{q}_{j,k,i}$, $\mathbf{q}_{k,i,j} = \mathbf{q}_{k,j,i}$, the contribution to potential energy will be rewritten as: $\frac{1}{3}[\varphi_3(|\mathbf{q}_{i,j,k}|) + \varphi_3(|\mathbf{q}_{j,k,i}|) + \varphi_3(|\mathbf{q}_{k,i,j}|)]$. Since the identity is true: $\mathbf{q}_{i,j,k} + \mathbf{q}_{j,k,i} + \mathbf{q}_{k,i,j} = \mathbf{0}$, from the three vectors $\mathbf{q}_{i,j,k}$, $\mathbf{q}_{j,k,i}$, $\mathbf{q}_{k,i,j}$ two are independent.

As a result, we can write the following representation for a three-particle potential:

$$U_3 = \frac{1}{6}\sum_{i,j,k=1\ (i\neq j\neq k\neq i)}^{N} \frac{1}{3}[\varphi_3(|\mathbf{q}_{i,j,k}|) + \varphi_3(|\mathbf{q}_{j,k,i}|) + \varphi_3(|\mathbf{q}_{k,i,j}|)] = \\ = \sum_{i<j<k} \frac{1}{3}[\varphi_3(|\mathbf{q}_{i,j,k}|) + \varphi_3(|\mathbf{q}_{j,k,i}|) + \varphi_3(|\mathbf{q}_{k,i,j}|)]. \quad (3)$$

After determining the binary (2) and three-particle (3) potentials, the algorithm for constructing all further multiparticle representations of the potential energy function $U_4, \ldots, U_N$ became clear. Below we will consider in more detail the multiparticle potential of the maximum particle, U_N.

Let us define a set of vectors $\mathbf{q}_i = \mathbf{r}_i - \frac{1}{N}\sum_{j=1}^{N}\mathbf{r}_j = \mathbf{r}_i - \mathbf{r}_{cs} = \frac{1}{N}\left[(N-1)\mathbf{r}_i - \sum_{j=1\ (j\neq i)}^{N}\mathbf{r}_j\right]$, where the $\mathbf{r}_{cs}$ — center of symmetry of the entire cluster, $i = 1, \ldots, N$. As in the cases of binary and three-particle potentials, a set of vectors $\mathbf{q}_1, \ldots, \mathbf{q}_N$ is directed from the center of symmetry of the cluster to each of the particles with the corresponding number. As a result, we will write down the desired expression:

$$U_N = \frac{1}{N}[\varphi_N(|\mathbf{q}_1|) + \cdots + \varphi_N(|\mathbf{q}_N|)] = \frac{1}{N}\sum_{i=1}^{N}\varphi_N(|\mathbf{q}_i|), \quad (4)$$

where $\varphi_N(\cdot)$ — as yet undefined function of one variable.

We define the set of functions $\varphi_2, \ldots, \varphi_N$ by choosing one of the known binary potentials as a basis, for example, the Mie potential, ϕ_{Mie}. For the Mie potential, a pair of particles with radius vectors $\mathbf{r}_i$ and $\mathbf{r}_j$ gives a contribution to the potential energy in the amount of:

$$\phi_{\text{Mie}}(r_{i,j}) = \varepsilon\phi\left(\frac{r_{i,j}}{r_0}\right) = \frac{\varepsilon}{n-m}\left[m\left(\frac{r_0}{r_{i,j}}\right)^n - n\left(\frac{r_0}{r_{i,j}}\right)^m\right], \quad (5)$$

where $r_{i,j} = |\mathbf{r}_{i,j}| = \sqrt{(x_i - x_j)^2 + (y_i - y_j)^2 + (z_i - z_j)^2}$, $\phi(r) = \frac{m}{n-m}r^{-n} - \frac{n}{n-m}r^{-m}$, $n > m > 0$, $r_0 = \text{const} > 0$ — the abscissa of the minimum function ϕ_{Mie}, $-\varepsilon = \phi_{\text{Mie}}(r_0)$ — the interaction energy of a pair of particles at the minimum point.

To use the Mie potential in defining a set of functions $\varphi_2, \ldots, \varphi_N$ it is necessary to select the appropriate parameters ε and r_0 for each of the functions of the set $\varphi_2, \ldots, \varphi_N$. In other words, let us assume that

$$\varphi_\alpha(q_\sim) = \varepsilon_\alpha\phi\left(\frac{q_\sim}{q_{*,\alpha}}\right) = \frac{\varepsilon_\alpha}{n-m}\left[m\left(\frac{q_{*,\alpha}}{q_\sim}\right)^n - n\left(\frac{q_{*,\alpha}}{q_\sim}\right)^m\right], \quad \alpha = 2, \ldots, N, \quad (6)$$

where $q_\sim = |\mathbf{q}_{i,j}|, |\mathbf{q}_{i,j,k}|, \ldots; q_{*,\alpha}, \alpha = 2, \ldots, N$ — some set of parameters.

The assessment of a set of energy parameters $\varepsilon_2, \ldots, \varepsilon_N$ can be carried out in different ways. Thus, from the point of view of the Born – Oppenheimer decomposition, the interaction potential U can be represented by the sum $U = U_2 + \cdots + U_N$ of binary, three-particle and other multiparticle potentials, whose contribution to the total energy decreases rapidly with increasing index, i. e. $\varepsilon_2 \gg \gg \varepsilon_3 \gg \cdots \gg \varepsilon_N$. Another approach involves describing the initial cluster with one of the multiparticle potentials, starting with U_3. In this case, for evaluation ε_α, $\alpha = 3, \ldots, N$ we can reason as follows. We know the parameter $\varepsilon_2 = \varepsilon$ for particle pairs well. Taking into account (2)–(6), we write down the representation $U_\alpha = \varepsilon_\alpha \sum \varphi'_\alpha$, where $\varphi'_\alpha = \frac{\varphi_\alpha}{\varepsilon_\alpha}$, $\alpha = 2, \ldots, N$, then, assuming that $U_\alpha \cong U_2$, $\alpha = 3, \ldots, N$, we get an estimate $\varepsilon_\alpha = \varepsilon_2 \frac{\sum \varphi'_2}{\sum \varphi'_\alpha} = \varepsilon \frac{\sum \varphi'_2}{\sum \varphi'_\alpha}$, $\alpha = 3, \ldots, N$ for an unknown set of parameters.

Let us evaluate the set of parameters $q_{*,\alpha}$, $\alpha = 2, \ldots, N$. So, when $\alpha = 2$ we have $q_\sim = |\mathbf{q}_{i,j}| = \frac{1}{2} r_{i,j}$. In this case, it can be assumed that $q_{*,2} = \frac{1}{2} r_0$, then the equilibrium minimum distance between a pair of particles will become equal r_0, which is described by the Mie potential in the form (5).

Let it be now $\alpha = 3$, a $q_\sim = |\mathbf{q}_{i,j,k}|$. Taking into account Fig. 1, *b*, it is clear that when positioning three particles in the form of an equilateral triangle, we have $|\mathbf{q}_{i,j,k}| = |\mathbf{q}_{j,i,k}| = |\mathbf{q}_{k,i,j}|$. In this case, as it is easy to figure out, $q_{*,3} = \frac{1}{\sqrt{3}} r_0$, what corresponds to the radius of the circumscribed circle of an equilateral triangle.

Finally, for $\alpha = 4$, i. e., for a regular tetrahedron $q_{*,4} = \frac{\sqrt{6}}{4} r_0$, which corresponds to the radius of the described sphere of the tetrahedron. However, it remains to understand what $q_{*,\alpha}$ are equal to when $\alpha \geqslant 5$. In the future, without limiting generality, we will measure distances and energies in units r_0 and ε, respectively.

To find $q_{*,\alpha}$ at $\alpha \geqslant 5$ we minimize the following form $\Omega = \sum\limits_{1=i<j=\alpha} \left(r_{i,j} + r_{i,j}^{-1} \right)$, i. e. we solve the problem $\Omega \to \min$ by changing the positions of the cluster particles and then calculating the expression

$$q_{*,\alpha} = \frac{1}{\alpha} \sum_{i=1}^{\alpha} |\mathbf{r}_i - \mathbf{r}_{cs}|. \tag{7}$$

The choice of shape Ω is associated with the requirement that the particles in the cluster, on the one hand, be attracted to each other, while on the other hand, pairs of particles should not get too close. In connection with the last remark, it can be understood that asymptotically, with an increase in the number of particles in the cluster, the parameter $q_{*,\alpha}$ will be proportional to the value $\alpha^{1/3}$, i. e. $q_{*,\alpha} \propto \alpha^{1/3}$.

To minimize the shape Ω, we will solve the problem of gradient descent in the following form:

$$\begin{aligned}
\dot{x}_i &= -\frac{\partial \Omega}{\partial x_i} = -\sum_{k=1\ (k\neq i)}^{\alpha} \left(r_{i,k}^{-1} - r_{i,k}^{-3} \right) x_{i,k}, \\
\dot{y}_i &= -\frac{\partial \Omega}{\partial y_i} = -\sum_{k=1\ (k\neq i)}^{\alpha} \left(r_{i,k}^{-1} - r_{i,k}^{-3} \right) y_{i,k}, \\
\dot{z}_i &= -\frac{\partial \Omega}{\partial z_i} = -\sum_{k=1\ (k\neq i)}^{\alpha} \left(r_{i,k}^{-1} - r_{i,k}^{-3} \right) z_{i,k},
\end{aligned} \tag{8}$$

where $x_{i,k} = x_i - x_k$, $y_{i,k} = y_i - y_k$, $z_{i,k} = z_i - z_k$, $i, k = 1, \ldots, \alpha$, the dot above the values denotes the derivative of the parameter that provides gradient descent. The system 3α of differential equations (8) is solved until the norm of the gradient of the potential energy function $\| \operatorname{grad} \Omega \| = \left(\sum\limits_{i=1}^{\alpha} \Omega_{x_i}^2 + \sum\limits_{i=1}^{\alpha} \Omega_{y_i}^2 + \sum\limits_{i=1}^{\alpha} \Omega_{z_i}^2 \right)^{1/2}$ becomes less than some small number δ equal to, for example, 10^{-10}, i. e., the completion of calculations of the system of differential equations is carried out provided that $\| \operatorname{grad} \Omega \| < \delta$.

To verify that the solution of problem (8) led to finding exactly the minimum configuration, it remains to find all the eigenvalues of the corresponding Hesse matrix H of the form Ω and ensure that all of them are non-negative. The Hesse matrix has dimensions $3\alpha \times 3\alpha$ and consists of nine cells $\left\{\Omega_{x_i,x_j}\right\}, \ldots, \left\{\Omega_{z_i,z_j}\right\}$, each of which has a size $\alpha \times \alpha$, because $i,\ j = 1, \ldots, \alpha$, i. e.,

$$H = \begin{bmatrix} \left\{\Omega_{x_i,x_j}\right\} & \left\{\Omega_{x_i,y_j}\right\} & \left\{\Omega_{x_i,z_j}\right\} \\ \left\{\Omega_{y_i,x_j}\right\} & \left\{\Omega_{y_i,y_j}\right\} & \left\{\Omega_{y_i,z_j}\right\} \\ \left\{\Omega_{z_i,x_j}\right\} & \left\{\Omega_{z_i,y_j}\right\} & \left\{\Omega_{z_i,z_j}\right\} \end{bmatrix}. \tag{9}$$

Below are all the necessary second partial derivatives of the form Ω, namely

$$\Omega_{x_i,x_j} = \delta_{i,j} \sum_{k\neq i} \left[\left(-r_{i,k}^{-3} + 3r_{i,k}^{-5}\right) x_{i,k}^2 + r_{i,k}^{-1} - r_{i,k}^{-3}\right] - (1-\delta_{i,j}) \left[\left(-r_{i,j}^{-3} + 3r_{i,j}^{-5}\right) x_{i,j}^2 + r_{i,j}^{-1} - r_{i,j}^{-3}\right],$$

$$\Omega_{x_i,y_j} = \delta_{i,j} \sum_{k\neq i} \left(-r_{i,k}^{-3} + 3r_{i,k}^{-5}\right) x_{i,k} y_{i,k} - (1-\delta_{i,j}) \left(-r_{i,j}^{-3} + 3r_{i,j}^{-5}\right) x_{i,j} y_{i,j},$$

$$\Omega_{x_i,z_j} = \delta_{i,j} \sum_{k\neq i} \left(-r_{i,k}^{-3} + 3r_{i,k}^{-5}\right) x_{i,k} z_{i,k} - (1-\delta_{i,j}) \left(-r_{i,j}^{-3} + 3r_{i,j}^{-5}\right) x_{i,j} z_{i,j},$$

$$\Omega_{y_i,x_j} = \delta_{i,j} \sum_{k\neq i} \left(-r_{i,k}^{-3} + 3r_{i,k}^{-5}\right) y_{i,k} x_{i,k} - (1-\delta_{i,j}) \left(-r_{i,j}^{-3} + 3r_{i,j}^{-5}\right) y_{i,j} x_{i,j},$$

$$\Omega_{y_i,y_j} = \delta_{i,j} \sum_{k\neq i} \left[\left(-r_{i,k}^{-3} + 3r_{i,k}^{-5}\right) y_{i,k}^2 + r_{i,k}^{-1} - r_{i,k}^{-3}\right] - (1-\delta_{i,j}) \left[\left(-r_{i,j}^{-3} + 3r_{i,j}^{-5}\right) y_{i,j}^2 + r_{i,j}^{-1} - r_{i,j}^{-3}\right],$$

$$\Omega_{y_i,z_j} = \delta_{i,j} \sum_{k\neq i} \left(-r_{i,k}^{-3} + 3r_{i,k}^{-5}\right) y_{i,k} z_{i,k} - (1-\delta_{i,j}) \left(-r_{i,j}^{-3} + 3r_{i,j}^{-5}\right) y_{i,j} z_{i,j},$$

$$\Omega_{z_i,x_j} = \delta_{i,j} \sum_{k\neq i} \left(-r_{i,k}^{-3} + 3r_{i,k}^{-5}\right) z_{i,k} x_{i,k} - (1-\delta_{i,j}) \left(-r_{i,j}^{-3} + 3r_{i,j}^{-5}\right) z_{i,j} x_{i,j},$$

$$\Omega_{z_i,y_j} = \delta_{i,j} \sum_{k\neq i} \left(-r_{i,k}^{-3} + 3r_{i,k}^{-5}\right) z_{i,k} y_{i,k} - (1-\delta_{i,j}) \left(-r_{i,j}^{-3} + 3r_{i,j}^{-5}\right) z_{i,j} y_{i,j},$$

$$\Omega_{z_i,z_j} = \delta_{i,j} \sum_{k\neq i} \left[\left(-r_{i,k}^{-3} + 3r_{i,k}^{-5}\right) z_{i,k}^2 + r_{i,k}^{-1} - r_{i,k}^{-3}\right] - (1-\delta_{i,j}) \left[\left(-r_{i,j}^{-3} + 3r_{i,j}^{-5}\right) z_{i,j}^2 + r_{i,j}^{-1} - r_{i,j}^{-3}\right],$$

where $\delta_{i,j}$ — the Kronecker symbol, $i,\ j,\ k = 1, \ldots, \alpha$.

Let us introduce a procedure for distinguishing two configurations from each other in a cluster of N identical particles. To do this, we will find all the binary distances $r_{i,j}$, $1 = i < j = N$ of the particles in the cluster. Such distances $N_b = \frac{1}{2}N(N-1)$. Let us order all binary distances in ascending order, to get a set of distances

$$R = \mathrm{sort}\{r_{1,2}, \ldots, r_{N-1,N}\} = \left\{\underbrace{r_{k_1,k_2}, \ldots, r_{l_1,l_2}}_{N_b}\right\},$$

where sort — the operation of sorting a set of numbers in ascending order.

Let us define the metric $d(\cdot,\cdot)$ in the space of all binary distances of the cluster under consideration as follows. Let there be a pair of configurations c_1, c_2 of cluster particles with sets of binary distances ordered in ascending order R_1, R_2, then the configurations c_1, c_2 are considered indistinguishable when $d(R_1, R_2) = \max\limits_{1\leqslant k\leqslant N_b} |R_{1,k} - R_{2,k}| \leqslant \delta_c$, where δ_c — some small number, otherwise we assume that the configurations are different. The proposed criterion is invariant with respect to shifts and rotations of the cluster in space, as well as with any permutation of particles in the cluster.

Let locally equilibrium configurations N_{lm} be found by solving the gradient descent problem (8), sets of ascending binary distances are calculated $R_1, \ldots, R_{N_{lm}}$. The algorithm for selecting a set $\left\{R_1, R_{i_2}, \ldots, R_{i_k}\right\}$ of configurations that do not match each other boils down to the following steps.

The desired set starts with the configuration R_1. If $d(R_2, R_1) > \delta_c$, then a second configuration is added to the desired set and $R_{i_2} = R_2$. Let us now consider R_3. To enable it, two inequalities must be fulfilled, provided that the configuration R_2 was enabled earlier, namely: $d(R_3, R_1) > \delta_c$, $d(R_3, R_2) > \delta_c$. Continuing the specified process of sorting through the locally available equilibrium configurations, we obtain the desired set of configurations $\left\{R_1, R_{i_2}, \ldots, R_{i_k}\right\}$ that do not match each other, which are located in pairs at a distance greater than δ_c. It can be verified that the space of configurations with distance $d(\cdot,\cdot)$ is a metric space. The fulfillment of the axioms of identity and symmetry is obvious, the fulfillment of the axiom of the triangle ($d(R_1, R_2) \leqslant d(R_1, R_3) + d(R_2, R_3)$) has been verified by the Monte Carlo method. In all experiments, the axiom of the triangle was fulfilled.

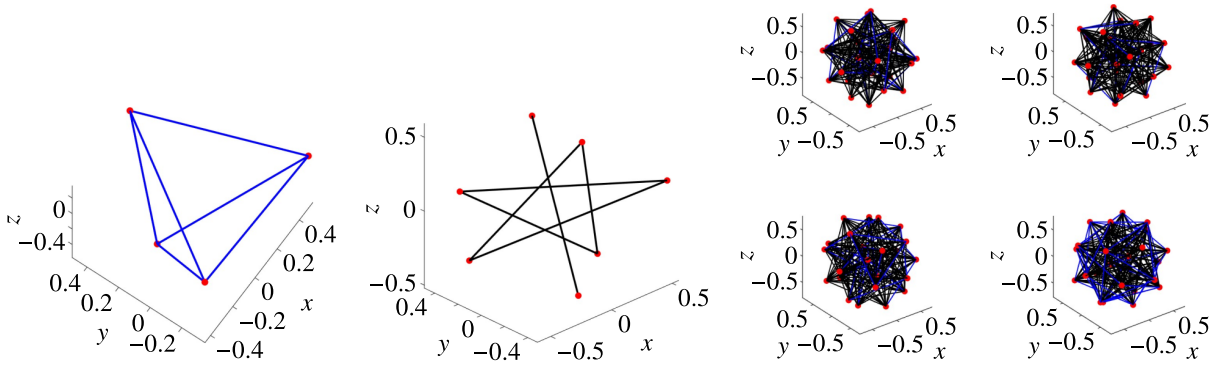

(a) Equilibrium configuration of particle positions at $\alpha = 4$

(b) Equilibrium configuration of particle positions at $\alpha = 7$

(c) Four locally equilibrium configurations of particle positions at $\alpha = 25$

Figure 2

Figure 2 shows examples of equilibrium and locally equilibrium configurations obtained by solving problem (8) in experiments with the number $M = 10^4$. In each of the experiments, all the eigenvalues of the Hesse matrix (9) were found, which turned out to be non-negative in all cases. In the calculations for solving problem (8), the initial positions of the cluster particles were selected uniformly randomly from a cube $[-L, L]^3$, where it was assumed that $L = 1$. In addition, it was assumed that $\delta = 10^{-10}$, $\delta_c = 0.05$. In Figure 2, the positions of the particles are indicated by red markers in the form of dots, the edges of blue and black colors have a length in the vicinity of one and from the interval [1, 2], respectively. It turned out that the solution of problem (8) with an increase in the number of particles in the cluster, starting from $\alpha = 9$, is not the only one. Figure 2, *c* shows four different configurations of particles in a cluster at $\alpha = 25$. In this case, when calculating by formula (7), it is necessary to average the number of locally equilibrium configurations.

Table 1. The dependence of the value $q_{*,\alpha}$ on α

α	2	3	4	5	6	7	8	12	20	25
$q_{*,\alpha}$	$\frac{1}{2} = 0.5$	$\frac{1}{\sqrt{3}} \cong 0.5774$	$\frac{\sqrt{6}}{4} \cong 0.6124$	0.6425	0.6593	0.6769	0.6888	0.7074	0.7364	0.7465

Table 1 shows the results of solving the problem (8) with subsequent estimation of the values $q_{*,\alpha}$ at $\alpha \geqslant 5$ according to the formula (7), as well as the known values at $\alpha = 2, 3, 4$. It should be noted that the exact values of the parameter $q_{*,\alpha}$ at $\alpha = 2, 3, 4$ are reproduced with high accuracy within the

framework of solving problem (8). According to Table 1, a suitable regression model of the dependence of the values $q_{*,\alpha}$ on α was constructed, namely $q_{*,\alpha} = 0.401 + 0.129\alpha^{1/3}$, at the same time, the coefficients of the regression model turned out to be significant at the level of no worse than $2 \cdot 10^{-4}$.

3. Marking up space using a binary potential

First, let us consider the binary interaction potential of particles in a cluster when $U = \sum\limits_{1 \leqslant i < j \leqslant N} \varphi_2(|\mathbf{q}_{i,j}|) = \sum\limits_{1 \leqslant i < j \leqslant N} \phi(|\mathbf{r}_{i,j}|)$, where $\phi(r) = \frac{\varepsilon}{n-m}\left[m\left(\frac{r_0}{r}\right)^n - n\left(\frac{r_0}{r}\right)^m\right]$. In units ε and r_0 the Mie potential can be rewritten in dimensionless form $\phi(r) = \frac{m}{n-m}r^{-n} - \frac{n}{n-m}r^{-m}$. Also, in the future we will need two derived functions $\phi(r)$: $\mu(r) = \frac{\phi'(r)}{r} = \frac{nm}{n-m}\left(-r^{-n-2} + r^{-m-2}\right)$ и $\chi(r) = \frac{\mu'(r)}{r} = \frac{n(n+2)m}{n-m}r^{-n-4} - \frac{nm(m+2)}{n-m}r^{-m-4}$. The specified binary potential in the form of Mie (Lennard – Jones) is used, for example, to describe noble (inert) gases [Hirschfelder, Curtiss, Bird, 1954].

Considering the particles in the cluster as balls with a radius $\frac{1}{2}r_0 = \frac{1}{2}$ and equating the volume of N ball particles to the volume of a cube with a side $2\left(L + \frac{1}{2}\right)$, we find $L = -\frac{1}{2} + \frac{1}{4}\sqrt[3]{\frac{4}{3}\pi N}$. In the future, when searching for stationary points of the potential energy function using the gradient descent method, we will proceed from the fact that the initial positions of the cluster particle centers are positioned inside the cube $[-L, L]^3$.

Taking into account the lower computational cost of searching for points of the local minimum of the potential energy function in comparison with other stationary points, we consider two computational procedures. As part of the first procedure for finding points of the local minimum, we will repeatedly solve the problem of gradient descent:

$$\begin{cases} \dot{x}_i = -U_{x_i} = -\sum\limits_{k \neq i} \mu(r_{i,k}) x_{i,k}, \\ \dot{y}_i = -U_{y_i} = -\sum\limits_{k \neq i} \mu(r_{i,k}) y_{i,k}, \\ \dot{z}_i = -U_{z_i} = -\sum\limits_{k \neq i} \mu(r_{i,k}) z_{i,k}, \end{cases} \tag{10}$$

where $i, k = 1, \ldots, N$; the point above the values x_i, y_i, z_i indicates the derivative of the variable along which the gradient descent is carried out. The system of $3N$ differential equations (10) is solved until the norm of the gradient of the potential energy function $\|\operatorname{grad} U\| = \left(\sum\limits_{i=1}^{N} U_{x_i}^2 + \sum\limits_{i=1}^{N} U_{y_i}^2 + \sum\limits_{i=1}^{N} U_{z_i}^2\right)^{1/2}$ becomes less than some small number δ.

To search for stationary points, including points of local minimum, we will minimize the expression $\Phi = \Phi(x_1, y_1, \ldots, z_N) = \frac{1}{2}\sum\limits_{i=1}^{N} U_{x_i}^2 + \frac{1}{2}\sum\limits_{i=1}^{N} U_{y_i}^2 + \frac{1}{2}\sum\limits_{i=1}^{N} U_{z_i}^2$. As a result, for the second computational procedure for finding stationary points using the gradient descent method, the following system of $3N$ ordinary differential equations can be written:

$$\begin{cases} \dot{x}_j = -\Phi_{x_j} = -\sum\limits_{i=1}^{N}\left(U_{x_i}U_{x_i,x_j} + U_{y_i}U_{y_i,x_j} + U_{z_i}U_{z_i,x_j}\right), \\ \dot{y}_j = -\Phi_{y_j} = -\sum\limits_{i=1}^{N}\left(U_{x_i}U_{x_i,y_j} + U_{y_i}U_{y_i,y_j} + U_{z_i}U_{z_i,y_j}\right), \\ \dot{z}_j = -\Phi_{z_j} = -\sum\limits_{i=1}^{N}\left(U_{x_i}U_{x_i,z_j} + U_{y_i}U_{y_i,z_j} + U_{z_i}U_{z_i,z_j}\right), \end{cases} \tag{11}$$

where $j = 1, \ldots, N$.

In (11) contains the elements of the Hesse matrix of the second derivatives of the potential energy function. A Hesse matrix having dimensions $3N \times 3N$, can be represented as a block matrix consisting of nine blocks $\left\{U_{x_i,x_j}\right\}, \ldots, \left\{U_{z_i,z_j}\right\}$, each of which has a size $N \times N$, because $i, j = 1, \ldots, N$, i. e.,

$$H = \begin{bmatrix} \left\{U_{x_i,x_j}\right\} & \left\{U_{x_i,y_j}\right\} & \left\{U_{x_i,z_j}\right\} \\ \left\{U_{y_i,x_j}\right\} & \left\{U_{y_i,y_j}\right\} & \left\{U_{y_i,z_j}\right\} \\ \left\{U_{z_i,x_j}\right\} & \left\{U_{z_i,y_j}\right\} & \left\{U_{z_i,z_j}\right\} \end{bmatrix}. \tag{12}$$

Below are the expressions for counting each of the nine block matrices included in (12):

$$U_{x_i,x_j} = \delta_{i,j} \sum_{k \neq i} \left[\chi(r_{i,k}) x_{i,k}^2 + \mu(r_{i,k})\right] - (1 - \delta_{i,j}) \left[\chi(r_{i,j}) x_{i,j}^2 + \mu(r_{i,j})\right],$$

$$U_{x_i,y_j} = \delta_{i,j} \sum_{k \neq i} \chi(r_{i,k}) x_{i,k} y_{i,k} - (1 - \delta_{i,j}) \chi(r_{i,j}) x_{i,j} y_{i,j},$$

$$U_{x_i,z_j} = \delta_{i,j} \sum_{k \neq i} \chi(r_{i,k}) x_{i,k} z_{i,k} - (1 - \delta_{i,j}) \chi(r_{i,j}) x_{i,j} z_{i,j},$$

$$U_{y_i,x_j} = \delta_{i,j} \sum_{k \neq i} \chi(r_{i,k}) y_{i,k} x_{i,k} - (1 - \delta_{i,j}) \chi(r_{i,j}) y_{i,j} x_{i,j},$$

$$U_{y_i,y_j} = \delta_{i,j} \sum_{k \neq i} \left[\chi(r_{i,k}) y_{i,k}^2 + \mu(r_{i,k})\right] - (1 - \delta_{i,j}) \left[\chi(r_{i,j}) y_{i,j}^2 + \mu(r_{i,j})\right],$$

$$U_{y_i,z_j} = \delta_{i,j} \sum_{k \neq i} \chi(r_{i,k}) y_{i,k} z_{i,k} - (1 - \delta_{i,j}) \chi(r_{i,j}) y_{i,j} z_{i,j},$$

$$U_{z_i,x_j} = \delta_{i,j} \sum_{k \neq i} \chi(r_{i,k}) z_{i,k} x_{i,k} - (1 - \delta_{i,j}) \chi(r_{i,j}) z_{i,j} x_{i,j},$$

$$U_{z_i,y_j} = \delta_{i,j} \sum_{k \neq i} \chi(r_{i,k}) z_{i,k} y_{i,k} - (1 - \delta_{i,j}) \chi(r_{i,j}) z_{i,j} y_{i,j},$$

$$U_{z_i,z_j} = \delta_{i,j} \sum_{k \neq i} \left[\chi(r_{i,k}) z_{i,k}^2 + \mu(r_{i,k})\right] - (1 - \delta_{i,j}) \left[\chi(r_{i,j}) z_{i,j}^2 + \mu(r_{i,j})\right].$$

First, we calculate the number of local minima N_{lm} of the potential energy function for a different number of particles in the cluster $N = 2, 3, \ldots$ For each N, task (10) is performed M times, counting the initial positions of the particles as uniformly random vectors in the cube $[-L, L]^3$.

Table 2 provides a summary of the results of calculating the number of local minima N_{lm} of the potential energy of the cluster with a different number of particles N. In all solutions of problem (10), it was assumed that $n = 12$, $m = 6$, i. e., the Lennard – Jones potential was taken into account. For each value of N, $M = 5 \times 10^4$ numerical solutions of the problem (10) were carried out. It was assumed that $\delta = 10^{-10}$, $\delta_c = 0.05$. The signs of the inequalities "⩾" in Table 2 mean that the estimates of the number of local minima are given from below.

Table 2. The results of calculating the number of local minima of potential energy for a different number of particles in a cluster

N	$2 \div 5$	6	7	8	12	15	20	25	30
N_{lm}	1	2	4	8	⩾ 290	⩾ 934	⩾ 6922	⩾ 16′423	⩾ 18′984

Table 2 clearly shows that the number of local minima N_{lm} increases rapidly with the increase of the number of particles N in the cluster. According to Table 2, we will construct an asymptotic

regression estimate $\left(\text{in the class of functions } N_{lm} = b_0 + e^{b_1 N}\right)$ of the number of local minima. It was found that the coefficient b_0 is not statistically significant (at the level of 0.05), whereas the coefficient b_1 is highly significant, therefore it can be written $N_{lm} \propto e^{0.327 \cdot N}$ at $N \geqslant 6$. The coefficient of 0.327 in the regression estimation is significant at the level of no worse then $5.56 \cdot 10^{-8}$. In other words, the number of local minima is growing exponentially fast. This assessment is consistent with the assessments of other authors [Stillinger, LaViolette, 1986; Бирштейн, Птицын, 1964].

Figure 3 shows spatial samples of locally equilibrium configurations of particles in clusters with a number of particles 6 and 7, respectively. The straight lines in the graphs in Figure 3 are drawn in cases where their length differs from one by no more than 0.05. The graphs in Figure 3 and below depict the potential energy values of each of the locally equilibrium configurations, ranked in ascending order of potential energy from left to right and from top to bottom.

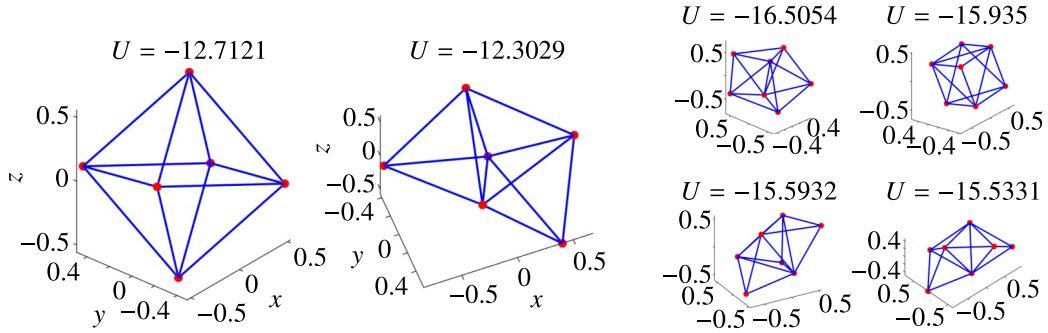

(a) Two locally equilibrium cluster configurations at $N = 6$

(b) Four locally equilibrium cluster configurations at $N = 7$

Figure 3

Let the values of potential energies of locally equilibrium configurations be concentrated in the interval $[\min U_{lm}, \max U_{lm}]$. In this case, the relative range of changes κ_{lm} in the potential energies of the equilibrium configurations is determined by the formula $\kappa_{lm} = \frac{2(\max U_{lm} - \min U_{lm})}{|\max U_{lm} + \min U_{lm}|}$. So for $N = 12$, 15, 20, 25, 30 it is found that $\kappa_{lm} = 0.1695$, 0.1479, 0.1346, 0.1042, 0.1000 respectively, i. e., with increasing N, the relative interval κ_{lm} decreases. Considering that the coefficient κ_{lm} is non-negative, a suitable regression formula was constructed to estimate the dependence κ_{lm} on N, namely $\kappa_{lm} = 0.054 + \frac{1.414}{N}$, $N \geqslant 12$ at a coefficient value level not higher than 0.012. Thus, with an exponential increase in the number of local minima, their relative energy concentration range decreases, i. e., there is a rapid increase in energy degeneracy of various local minima. This means that individual locally equilibrium spatial configurations can be very different, whereas their energies can be close to each other.

As an example, we will construct a pair of locally equilibrium cluster configurations with $N = 30$, which, on the one hand, are spatially noticeably different from each other, on the other hand, their energies differ slightly. Let the desired equilibrium configurations have numbers s and h. Let us determine the relative distance between the energies of the equilibrium configurations by the formula: $\kappa_{s,h} = \frac{2|U_{lm,s} - U_{lm,h}|}{|U_{lm,s} + U_{lm,h}|}$. We will assume that a certain set of locally equilibrium configurations has been found in M experiments on solving the system of equations (10). Let us choose from this set such a pair of configurations with numbers s and h, for which the maximum is realized $D = \max\limits_{s,h;\ \kappa_{s,h} \leqslant \delta_\kappa} d(R_s, R_h)$, when $\kappa_{s,h} \leqslant \delta_\kappa$.

Figure 4 shows the result of calculations in the form of a pair of locally equilibrium configurations that differ markedly from each other, whose energies differ slightly. Although it was believed that $M = 5 \cdot 10^4$, $\delta_\kappa = 10^{-4}$, it turned out that $D = 0.9899$, i. e., a pair of configurations are

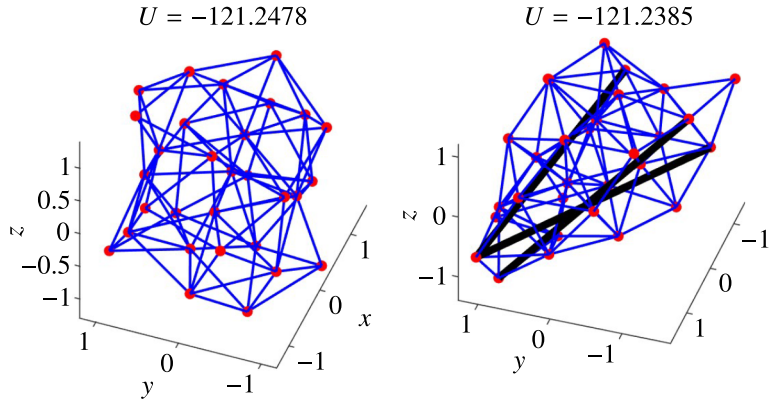

Figure 4. Example of a pair of markedly different locally equilibrium configurations of a cluster with $N = 30$, whose energies differ in the second decimal place

spatially noticeably distinguishable. To clearly indicate the difference between a pair of configurations, edges with lengths in the vicinity of one are marked in blue, while edges with lengths in the vicinity of 3.5 are marked in black. As indicated by the presence of several long black ribs, the configuration on the right in Figure 4 is noticeably more elongated than the configuration on the left.

Figure 5 shows two graphs describing the statistics of a population of 18′984 local minima of a cluster with $N = 30$ particles. A histogram of the distribution of local minima in energy is plotted on the left graph. A suitable density curve for the normal distribution is also shown. It can be seen that the envelope of the histogram differs slightly from the density of the normal distribution, having a noticeable positive coefficient of asymmetry. The right graph shows a diagram of the scattering of potential energies of locally equilibrium configurations of the cluster under consideration.

Table 3 provides a summary of the results of calculating the number of saddle configurations N_{sc} of the potential energy of the cluster with a different number of N particles. When numerically solving problem (11), it was assumed that $L = \frac{1}{4}\sqrt[3]{\frac{4}{3}\pi N}$, this is somewhat more than in previous calculations. In addition, in all calculations for different values of N, it was assumed that $M = 10^5$, $\delta = 10^{-10}$, $\delta_c = 0.05$.

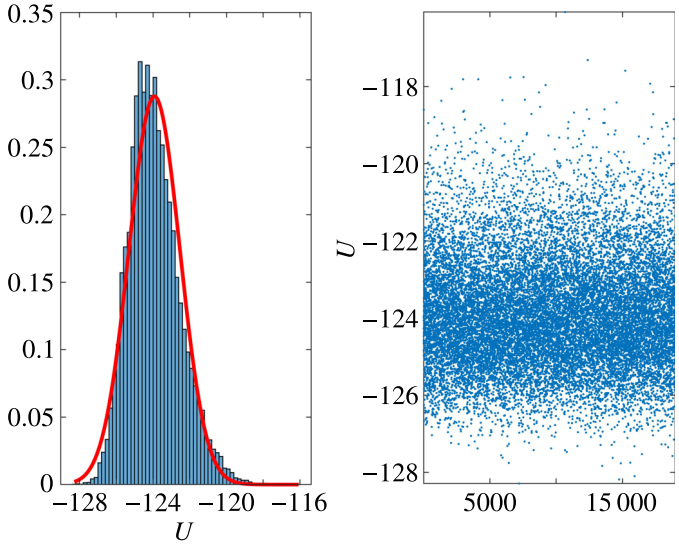

Figure 5. Histogram (left) and scatterplot (right) of energies of locally equilibrium configurations of cluster particles at $N = 30$

Table 3. The results of calculating the number of saddle configurations of potential energy for a different number of particles in a cluster

N	2	3	4	5	6	7	8	12
N_{sc}	—	2	4	15	$\geqslant 77$	$\geqslant 536$	$\geqslant 4557$	$\geqslant 86'423$

From a comparison of Table 3 with Table 2, it follows that the number of saddle configurations is growing even faster than the increase in the number of configurations of local minima with an increase in N. According to Table 3, a regression model was built to estimate the number of saddle configurations, namely $N_{sc} \propto e^{0.947 \cdot N}$, $N \geqslant 4$, whose coefficient is significant at the level of no worse then $2.22 \cdot 10^{-11}$. A comparison of the two regression models shows that the coefficients in exponents at N differ from each other by 2.90 times, i. e., roughly speaking, $N_{sc} \propto N_{lm}^{2.90}$.

Figure 6 shows the saddle configurations of two clusters with $N = 4$ and $N = 5$ particles in each. Note that all four saddle configurations of a cluster consisting of four particles are flat shapes.

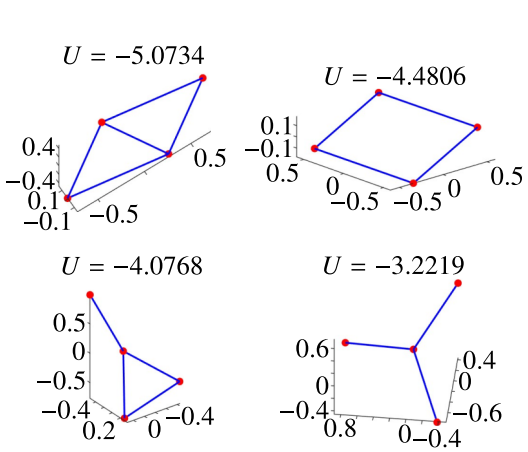

(a) All saddle configurations in a four-particle cluster, $N = 4$

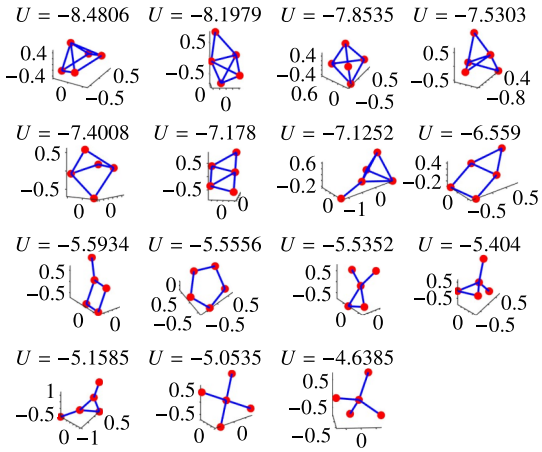

(b) All saddle configurations in a cluster with five particles, $N = 5$

Figure 6

As in the case of equilibrium configurations, the relative interval of change in the potential energies of saddle configurations κ_{sc}, calculated by the formula $\kappa_{sc} = \frac{2(\max U_{sc} - \min U_{sc})}{|\max U_{sc} + \min U_{sc}|}$ was estimated. It turned out that for $N = 4, 5, 6, 7, 8, 12$, the relative intervals of change in the energy of the saddle points were $\kappa_{sc} = 0.4464, 0.5857, 0.6544, 0.7018, 0.7835, 0.8152$. Based on these data, the regression dependence of the coefficient κ_{sc} on N. It turned out that $\kappa_{sc} = 1.034 - \frac{2.289}{N}$, $N \geqslant 4$, where a pair of coefficients of the regression model are significant at the level of no worse then $2.59 \cdot 10^{-4}$. Thus, the relative interval of change in the energy of saddle points with increasing N can be assumed to tend to a certain constant value.

Note that in the numerical solution of problem (11), it was not possible to detect the presence of local maxima in the Lennard – Jones binary potential. There were exclusively saddle configurations and configurations of local minima.

4. Conformational transitions with binary potential

Consider the joint positioning of equilibrium configurations and saddle configurations, for example, when $N = 7$. Taking into account Table 2 and Table 3 at $N = 7$, the number of equilibrium configurations will be $N_{lm} = 4$, while the number of saddle configurations will be — $N_{sc} = 536$.

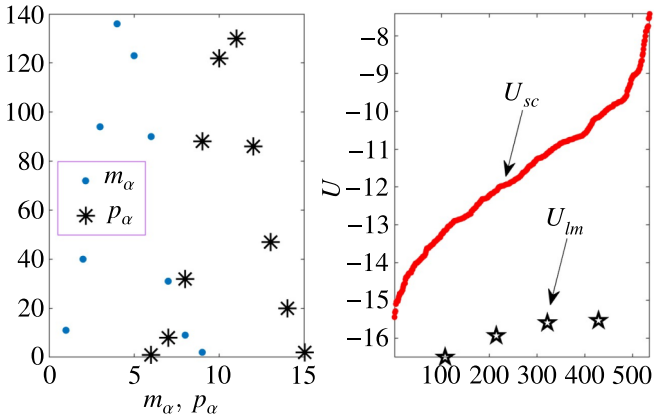

Figure 7. Distribution of the number of positive and negative eigenvalues of the Hesse matrix of saddle configurations (left); distributions of potential energies of saddle, U_{sc} and locally equilibrium configurations, U_{lm} (right)

Figure 7 on the left shows two distributions of the number of saddle points with the same values of the number of positive $p_\alpha = 6, \ldots, 14$ and negative $m_\alpha = 1, \ldots, 9$ eigenvalues of the Hesse matrix (12) for the selected number of particles in the cluster $N = 7$. Both distributions are symmetric, because the equality was true for each saddle configuration $p_\alpha + m_\alpha = 3N - 6|_{N=7} = 15$, $\alpha = 1, \ldots, 536$. Figure 7 on the right shows the distributions of potential energies of saddle (U_{sc}, markers in the form of dots) and locally equilibrium configurations (U_{lm}, markers in the form of pentagrams). It can be clearly seen that the potential energies of locally equilibrium configurations lie below the corresponding energies of saddle configurations. For convenience, all potential energies in groups of saddle and locally equilibrium configurations are subordinated in ascending order.

Let us consider the question of the transformation of an arbitrary saddle configuration into one or another equilibrium configuration, bearing in mind the effect of a force equal to the anti-gradient of potential energy. We will denote by w_i, $i = 1, \ldots, N_{lm} = 4$ the number of saddle configurations, which, after some variation of the initial configuration, under the action of an anti-gradient of potential energy, turn into one, two, etc. equilibrium configurations. By some variation of the initial configuration, it is understood that a small random vector $\theta\{\xi_1, \ldots, \xi_{3N}\}$ was added to the saddle configuration $\left\{x_1^{(sc)}, \ldots, z_N^{(sc)}\right\}$. Wherein it is considered that $\theta = 0.05$ and a set $\xi_1, \ldots, \xi_{3N}$ — uniformly random numbers from the interval $[-1, 1]$. The number of variations of saddle configurations was chosen in proportion to the value $250p_\alpha$, $\alpha = 1, \ldots, N_{sc} = 536$ and varied from $250 \times 6 = 1500$ to $250 \times 14 = 3500$. After each variation, gradient descent was applied by solving problem (10), followed by reaching one of the four equilibrium configurations.

Figure 8 shows a typical calculation sample in the form of four graphs, on which straight lines connect saddle and equilibrium configurations in four cases when one, two, three and four equilibrium configurations are achievable from the saddle point, respectively. For this calculation, the number of corresponding saddle configurations was: $w_1 = 26$, $w_2 = 102$, $w_3 = 194$, $w_4 = 214$, at the same time $w_1 + w_2 + w_3 + w_4 = 536$. From the analysis of numerical frequency values, it can be seen that the proportion of saddle configurations, of which a single equilibrium configuration is achievable, is a small value $\approx 4.8\,\%$. Of the majority of saddle points ($\approx 76.1\,\%$) three and four equilibrium configurations are achievable. As in Figure 7, in Figure 8, saddle configurations are marked with markers in the form of dots, while locally equilibrium configurations are marked with markers in the form of pentagrams.

We will define and study the mechanism of transformation of the cluster geometry, similar to conformational fluctuations. The conformations of macromolecules were considered earlier [Бирштейн, Птицын, 1964]; currently this direction is under intensively developing in the context of computational experimentation [Chakraborty, Banerjee, Wales, 2021].

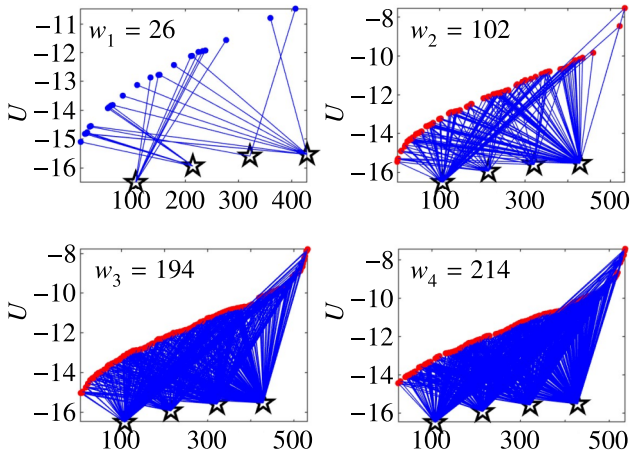

Figure 8. Ways of achieving equilibrium configurations from each saddle configuration in a cluster with $N = 7$

Let the excitation energy ΔE be transferred in some way to a locally equilibrium cluster lm_0, initially having one of the equilibrium configurations with energy U_{lm_0}. The new energy of the cluster $U_{lm_0} + \Delta E$ should enter the range $[\min U_{sc}, \max U_{sc}]$, i. e. $U_{lm_0} + \Delta E \in [\min U_{sc}, \max U_{sc}]$. Taking into account Figure 8, it is clear that the energy range $[\min U_{sc}, \max U_{sc}]$ is densely filled with various saddle configurations. Let the new cluster configuration sc_1 coincide with such a saddle configuration, whose energy is closest to the energy $U_{lm_0} + \Delta E$, i. e. $U_{sc_1} \cong U_{lm_0} + \Delta E$. For the transition from the saddle configuration $sc_1 = \left\{x_1^{(1)}, \ldots, z_N^{(1)}\right\}$ to one of the locally equilibrium configurations, problem (10) was solved, while randomly perturbed positions of the saddle configuration were selected as initial positions according to the formula: $\left\{x_1^{(1)} + \theta\xi_1, \ldots, z_N^{(1)} + \theta\xi_{3N}\right\}$, where $\theta = 0.05$, $\xi_1, \ldots, \xi_{3N}$ are uniformly random numbers from the segment $[-1, 1]$. After entering one of the equilibrium configurations lm_1 with energy U_{lm_1}, the whole procedure was repeated. As a result, a chain of conformational transitions was built: $lm_0 \to sc_1 \to lm_1 \to sc_2 \to \ldots$ The number of different saddle configurations, which did not exceed the number of equilibrium configurations, amounted to the number four for this particular case.

Figure 9 shows typical results of a computational experiment illustrating various formats of conformational transitions in the form of "switches". A switch is understood as a nonstationary conformational oscillation in which equilibrium and saddle configurations from fixed sets are quasi-periodically repeated. An arbitrary switch $S_{p,q}$ can be characterized by a pair of integers, where is the number of equilibrium and saddle configurations p ($p \geqslant 1$) and q ($q \geqslant 1$) manifested in a conformational oscillation.

The thickness of the arrows in Figure 9 illustrates the frequency of transition between cluster configurations in a chain of conformational transitions, whose length in all calculations was 300. There are also geometric miniatures of clusters in saddle (top) and locally equilibrium (bottom) formats.

Figures 9, *a* and 9, *b* shows the switches $S_{1,2}$ and $S_{2,2}$. At the same time, if in Figure 9, *a* both locally equilibrium positions are achievable from one saddle configuration, then in the example in Figure 9, *b* is from two. Finally, Figures 9, *c* and 9, *d* show examples of switches $S_{3,2}$, $S_{4,4}$.

5. Marking space using a multiparticle potential

Let us consider the marking of space using a multiparticle potential U_N with maximum partiality. Taking into account (4), (5), we write down the desired potential:

$$U_N = \frac{1}{N}\sum_{i=1}^{N}\varphi_N(q_i) = \frac{\varepsilon_N}{N}\sum_{i=1}^{N}\phi\left(\frac{q_i}{q_{*,N}}\right), \tag{13}$$

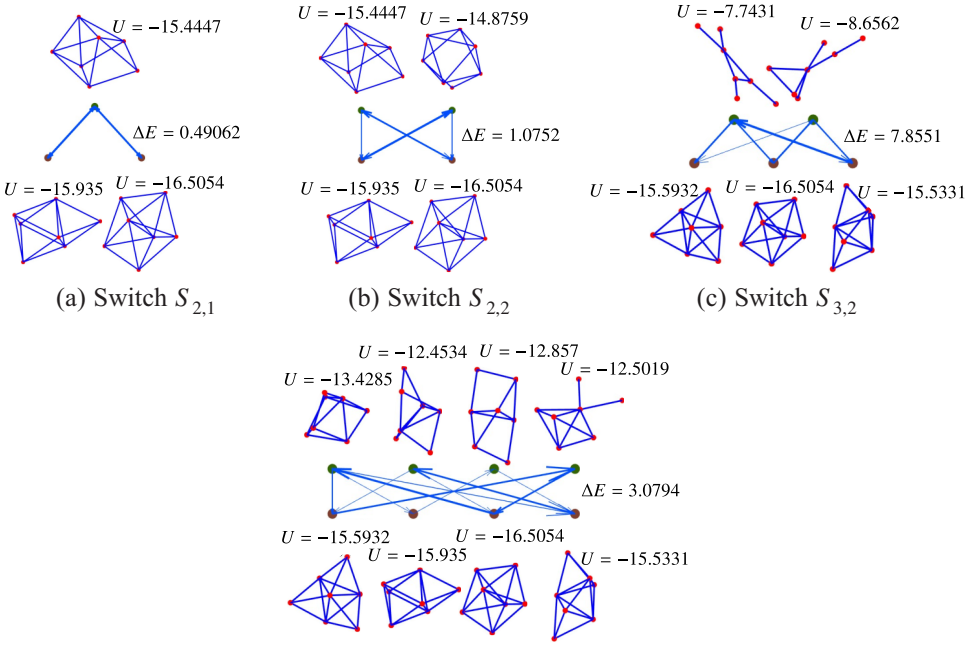

(a) Switch $S_{2,1}$ (b) Switch $S_{2,2}$ (c) Switch $S_{3,2}$

(d) Switch $S_{4,4}$

Figure 9

where $\phi(r) = \frac{m}{n-m} r^{-n} - \frac{n}{n-m} r^{-m}$, $q_i = |\mathbf{q}_i|$, $\mathbf{q}_i = \mathbf{r}_i - \mathbf{r}_{cs}$, $\mathbf{r}_{cs} = \frac{1}{N} \sum\limits_{j=1}^{N} \mathbf{r}_j$ — the center of symmetry of the cluster particles. The parameter estimation $q_{*,N}$ is given in the second section, namely $q_{*,N} = 0.401 + 0.129N^{1/3}$.

Let us define the procedure for searching for equilibrium configurations of cluster particles with potential energy (13) by the gradient descent method, then

$$\begin{aligned}
\dot{x}_i &= -\frac{\partial U_N}{\partial x_i} = -\frac{\varepsilon_N}{N q_{*,N}^2} \left[\mu\left(\frac{q_i}{q_{*,N}}\right)(x_i - x_{cs}) - \frac{1}{N} \sum_{k=1}^{N} \mu\left(\frac{q_k}{q_{*,N}}\right)(x_k - x_{cs}) \right], \\
\dot{y}_i &= -\frac{\partial U_N}{\partial y_i} = -\frac{\varepsilon_N}{N q_{*,N}^2} \left[\mu\left(\frac{q_i}{q_{*,N}}\right)(y_i - y_{cs}) - \frac{1}{N} \sum_{k=1}^{N} \mu\left(\frac{q_k}{q_{*,N}}\right)(y_k - y_{cs}) \right], \\
\dot{z}_i &= -\frac{\partial U_N}{\partial z_i} = -\frac{\varepsilon_N}{N q_{*,N}^2} \left[\mu\left(\frac{q_i}{q_{*,N}}\right)(z_i - z_{cs}) - \frac{1}{N} \sum_{k=1}^{N} \mu\left(\frac{q_k}{q_{*,N}}\right)(z_k - z_{cs}) \right],
\end{aligned} \tag{14}$$

where $\mu(r) = \frac{\phi'(r)}{r} = \frac{nm}{n-m}\left(-r^{-n-2} + r^{-m-2}\right)$, it was believed that $n = 12$, $m = 6$.

A new quality was found when estimating the number of locally equilibrium configurations in the multiparticle potential (13) by repeatedly solving the system of equations (14) at different values of the number of particles in the cluster N. Starting from the value $N = 4$, the number of equilibrium configurations turned out to be infinite, while they are not separated from each other. It also turned out that the energy of each of the equilibrium configurations is the same and equal $-\varepsilon_N$. In the calculations, it was assumed that $\varepsilon_N = 1$. Below we show that all equilibrium configurations in the face of the positions of the cluster particles are located on a sphere, whose center corresponds to the center of symmetry of the cluster, while the radius of the sphere is equal to $q_{*,N}$.

To illustrate the existence of an infinite number of equilibrium configurations, a series of calculations of the system of equations (14) was performed to find the number of equilibrium

configurations N_{lm} in a cluster of four particles, i. e., at $N = 4$. The parameter δ_c that separated one equilibrium configuration from another varied within the framework of the corresponding criterion.

In all calculations, the initial positions of the cluster particles were selected uniformly randomly from the cube $[-L, L]^3$, where it was assumed that $L = -\frac{1}{2} + \frac{1}{4}\sqrt[3]{\frac{4}{3}\pi N}$. The number of calculations M of the system of equations (13) for each of the parameter values δ_c was chosen equal 10^4. The parameter δ in the gradient descent completion criteria was considered as equal to 10^{-10}. According to Table 4, the number of equilibrium configurations increases rapidly with decreasing parameter δ_c. This indicates that there are infinitely many equilibrium configurations, which are not separated from each other. Thus, unlike the binary potential, where the equilibrium configurations are separated from each other, there are infinitely many nonseparated equilibrium configurations in the multiparticle potential.

Table 4. Dependence of the number of equilibrium configurations in a cluster with $N = 4$ on the parameter δ_c

δ_c	0.05	0.02	10^{-2}	10^{-3}
N_{lm}	25	114	386	7382

We illustrate the positioning of an infinite number of equilibrium configurations of a multiparticle potential on the surface of a sphere with a radius $q_{*,N}$, whose center coincides with the center of symmetry of the cluster. Let us make up the abbreviation of Lomonosov Moscow State University — MSU from the positions of $N = 114$ cluster particles. Let us ensure that this, when chosen as the initial configuration, leads to an equilibrium configuration obtained as a result of solving the system of equations (14). Figure 10 shows the result in the form of a sphere of radius $q_{*,N}$, on whose surface the points indicate the positions of the first 57 particles (Figure 10, *a*) and the second 57 (Figure 10, *b*), the positions of which are distinguished by a sign. Straight lines connect the vertices, the distance between which is in the vicinity of 0.1463.

(a) The locally equilibrium configuration of $N = 114$ particles, the positions of 57 of which reproduce the abbreviation MSU

(b) The locally equilibrium configuration of $N = 114$ particles, the positions of 57 of which reproduce the inverted abbreviation MSU

Figure 10

We define a procedure for searching for stationary (saddle) configurations of cluster particles with potential energy (13) by the gradient descent method. To do this, we will solve the problem (11), (12), where we take the multiparticle potential (13) as a potential. Let us write down the expressions for the nine blocks of the Hesse matrix (12) of the multiparticle potential (13); then

$$\frac{\partial^2 U_N}{\partial x_i \partial x_j} = \frac{\varepsilon_N}{N q_{*,N}^2}\left\{\left[\frac{1}{q_{*,N}^2}\chi\left(\frac{q_i}{q_{*,N}}\right)(x_i - x_{cs})^2 + \mu\left(\frac{q_i}{q_{*,N}}\right)\right]\delta_{i,j} - \frac{1}{N q_{*,N}^2}\chi\left(\frac{q_i}{q_{*,N}}\right)(x_i - x_{cs})^2 - \right.$$
$$\left. - \frac{1}{N}\mu\left(\frac{q_i}{q_{*,N}}\right) - \frac{1}{N q_{*,N}^2}\chi\left(\frac{q_j}{q_{*,N}}\right)(x_j - x_{cs})^2 - \frac{1}{N}\mu\left(\frac{q_j}{q_{*,N}}\right) + \right.$$

$$+\frac{1}{N^2 q_{*,N}^2}\sum_k \chi\left(\frac{q_k}{q_{*,N}}\right)(x_k - x_{cs})^2 + \frac{1}{N^2}\sum_k \mu\left(\frac{q_k}{q_{*,N}}\right)\Bigg\},$$

$$\frac{\partial^2 U_N}{\partial x_i\,\partial y_j} = \frac{\varepsilon_N}{N q_{*,N}^2}\left[\frac{1}{q_{*,N}^2}\chi\left(\frac{q_i}{q_{*,N}}\right)(x_i - x_{cs})(y_i - y_{cs})\delta_{i,j} - \frac{1}{N q_{*,N}^2}\chi\left(\frac{q_i}{q_{*,N}}\right)(x_i - x_{cs})(y_i - y_{cs}) - \right.$$
$$- \frac{1}{N q_{*,N}^2}\chi\left(\frac{q_j}{q_{*,N}}\right)(x_j - x_{cs})(y_j - y_{cs}) + \frac{1}{N^2 q_{*,N}^2}\sum_k \chi\left(\frac{q_k}{q_{*,N}}\right)(x_k - x_{cs})(y_k - y_{cs}) +$$
$$\left.+\frac{1}{N^2}\sum_k \mu\left(\frac{q_k}{q_{*,N}}\right)\right],$$

$$\frac{\partial^2 U_N}{\partial x_i\,\partial z_j} = \frac{\varepsilon_N}{N q_{*,N}^2}\left[\frac{1}{q_{*,N}^2}\chi\left(\frac{q_i}{q_{*,N}}\right)(x_i - x_{cs})(z_i - z_{cs})\delta_{i,j} - \frac{1}{N q_{*,N}^2}\chi\left(\frac{q_i}{q_{*,N}}\right)(x_i - x_{cs})(z_i - z_{cs}) - \right.$$
$$- \frac{1}{N q_{*,N}^2}\chi\left(\frac{q_j}{q_{*,N}}\right)(x_j - x_{cs})(z_j - z_{cs}) + \frac{1}{N^2 q_{*,N}^2}\sum_k \chi\left(\frac{q_k}{q_{*,N}}\right)(x_k - x_{cs})(z_k - z_{cs}) +$$
$$\left.+\frac{1}{N^2}\sum_k \mu\left(\frac{q_k}{q_{*,N}}\right)\right],$$

$$\frac{\partial^2 U_N}{\partial y_i\,\partial x_j} = \frac{\varepsilon_N}{N q_{*,N}^2}\left[\frac{1}{q_{*,N}^2}\chi\left(\frac{q_i}{q_{*,N}}\right)(y_i - y_{cs})(x_i - x_{cs})\delta_{i,j} - \frac{1}{N q_{*,N}^2}\chi\left(\frac{q_i}{q_{*,N}}\right)(y_i - y_{cs})(x_i - x_{cs}) - \right.$$
$$- \frac{1}{N q_{*,N}^2}\chi\left(\frac{q_j}{q_{*,N}}\right)(y_j - y_{cs})(x_j - x_{cs}) + \frac{1}{N^2 q_{*,N}^2}\sum_k \chi\left(\frac{q_k}{q_{*,N}}\right)(y_k - y_{cs})(x_k - x_{cs}) +$$
$$\left.+\frac{1}{N^2}\sum_k \mu\left(\frac{q_k}{q_{*,N}}\right)\right],$$

$$\frac{\partial^2 U_N}{\partial y_i\,\partial y_j} = \frac{\varepsilon_N}{N q_{*,N}^2}\left\{\left[\frac{1}{q_{*,N}^2}\chi\left(\frac{q_i}{q_{*,N}}\right)(y_i - y_{cs})^2 + \mu\left(\frac{q_i}{q_{*,N}}\right)\right]\delta_{i,j} - \frac{1}{N q_{*,N}^2}\chi\left(\frac{q_i}{q_{*,N}}\right)(y_i - y_{cs})^2 - \frac{1}{N}\mu\left(\frac{q_i}{q_{*,N}}\right) - \right.$$
$$- \frac{1}{N q_{*,N}^2}\chi\left(\frac{q_j}{q_{*,N}}\right)(y_j - y_{cs})^2 - \frac{1}{N}\mu\left(\frac{q_j}{q_{*,N}}\right) + \frac{1}{N^2 q_{*,N}^2}\sum_k \chi\left(\frac{q_k}{q_{*,N}}\right)(y_k - y_{cs})^2 +$$
$$\left.+\frac{1}{N^2}\sum_k \mu\left(\frac{q_k}{q_{*,N}}\right)\right\},$$

$$\frac{\partial^2 U_N}{\partial y_i\,\partial z_j} = \frac{\varepsilon_N}{N q_{*,N}^2}\left[\frac{1}{q_{*,N}^2}\chi\left(\frac{q_i}{q_{*,N}}\right)(y_i - y_{cs})(z_i - z_{cs})\delta_{i,j} - \frac{1}{N q_{*,N}^2}\chi\left(\frac{q_i}{q_{*,N}}\right)(y_i - y_{cs})(z_i - z_{cs}) - \right.$$
$$- \frac{1}{N q_{*,N}^2}\chi\left(\frac{q_j}{q_{*,N}}\right)(y_j - y_{cs})(z_j - z_{cs}) + \frac{1}{N^2 q_{*,N}^2}\sum_k \chi\left(\frac{q_k}{q_{*,N}}\right)(y_k - y_{cs})(z_k - z_{cs}) +$$
$$\left.+\frac{1}{N^2}\sum_k \mu\left(\frac{q_k}{q_{*,N}}\right)\right],$$

$$\frac{\partial^2 U_N}{\partial z_i\,\partial x_j} = \frac{\varepsilon_N}{N q_{*,N}^2}\left[\frac{1}{q_{*,N}^2}\chi\left(\frac{q_i}{q_{*,N}}\right)(z_i - z_{cs})(x_i - x_{cs})\delta_{i,j} - \frac{1}{N q_{*,N}^2}\chi\left(\frac{q_i}{q_{*,N}}\right)(z_i - z_{cs})(x_i - x_{cs}) - \right.$$

$$- \frac{1}{Nq_{*,N}^2}\chi\left(\frac{q_j}{q_{*,N}}\right)(z_j - z_{cs})(x_j - x_{cs}) + \frac{1}{N^2 q_{*,N}^2}\sum_k \chi\left(\frac{q_k}{q_{*,N}}\right)(z_k - z_{cs})(x_k - x_{cs}) +$$

$$+\frac{1}{N^2}\sum_k \mu\left(\frac{q_k}{q_{*,N}}\right)\Bigg],$$

$$\frac{\partial^2 U_N}{\partial z_i \partial y_j} = \frac{\varepsilon_N}{Nq_{*,N}^2}\left[\frac{1}{q_{*,N}^2}\chi\left(\frac{q_i}{q_{*,N}}\right)(z_i - z_{cs})(y_i - y_{cs})\delta_{i,j} - \frac{1}{Nq_{*,N}^2}\chi\left(\frac{q_i}{q_{*,N}}\right)(z_i - z_{cs})(y_i - y_{cs}) -\right.$$

$$- \frac{1}{Nq_{*,N}^2}\chi\left(\frac{q_j}{q_{*,N}}\right)(z_j - z_{cs})(y_j - y_{cs}) + \frac{1}{N^2 q_{*,N}^2}\sum_k \chi\left(\frac{q_k}{q_{*,N}}\right)(z_k - z_{cs})(y_k - y_{cs}) +$$

$$+\frac{1}{N^2}\sum_k \mu\left(\frac{q_k}{q_{*,N}}\right)\Bigg],$$

$$\frac{\partial^2 U_N}{\partial z_i \partial z_j} = \frac{\varepsilon_N}{Nq_{*,N}^2}\left\{\left[\frac{1}{q_{*,N}^2}\chi\left(\frac{q_i}{q_{*,N}}\right)(z_i - z_{cs})^2 + \mu\left(\frac{q_i}{q_{*,N}}\right)\right]\delta_{i,j} - \frac{1}{Nq_{*,N}^2}\chi\left(\frac{q_i}{q_{*,N}}\right)(z_i - z_{cs})^2 - \frac{1}{N}\mu\left(\frac{q_i}{q_{*,N}}\right) -\right.$$

$$- \frac{1}{Nq_{*,N}^2}\chi\left(\frac{q_j}{q_{*,N}}\right)(z_j - z_{cs})^2 - \frac{1}{N}\mu\left(\frac{q_j}{q_{*,N}}\right) + \frac{1}{N^2 q_{*,N}^2}\sum_k \chi\left(\frac{q_k}{q_{*,N}}\right)(z_k - z_{cs})^2 +$$

$$+\frac{1}{N^2}\sum_k \mu\left(\frac{q_k}{q_{*,N}}\right)\Bigg\},$$

where $\chi(r) = \frac{\mu'(r)}{r} = \frac{n(n+2)m}{n-m}r^{-n-4} - \frac{nm(m+2)}{n-m}r^{-m-4}$.

Table 5. Dependence of the number of saddle configurations in a cluster with $N = 4$ on the parameter δ_c

δ_c	0.05	0.02	10^{-2}	10^{-3}
N_{sc}	337	1235	2811	9324

As it turned out, as a result of solving problem (11), (12) with potential (13) at $N = 4$, the number of saddle points is infinite. To illustrate the latter statement, Table 5 shows the results of a computational experiment on counting the number of saddle points N_{sc} by solving problem (11)–(13).

In all calculations, the initial positions of the cluster particles were selected uniformly randomly from the cube $[-L, L]^3$, where it was assumed that $L = \frac{1}{4}\sqrt[3]{\frac{4}{3}\pi N}$. The number of calculations M of the system of equations (11)–(13) for each of the parameter values δ_c was chosen equal 10^4. The parameter δ in the gradient descent completion criteria was considered equal 10^{-4}. According to Table 5, the number of saddle configurations is growing rapidly with decreasing parameter δ_c. This indicates that there are infinitely many saddle configurations and that they are not separated from each other. As a criterion for the selection of saddle stationary points, the number of negative eigenvalues of the Hesse matrix of potential energy (12) at a stationary point was calculated; this number should be greater than zero.

To illustrate the positioning of saddle points relative to a sphere (radius $q_{*,N}$), on which locally equilibrium configurations of potential energy (13) are concentrated, a cluster with $N = 50$ was considered. The search for saddle stationary points in the cluster was carried out in a series of $M = 200$ computational experiments to solve the problem (11)–(13). The choice of the remaining parameter values, including the choice of the initial positioning of the cluster particles, corresponded to the choice of the parameter values of the previous task.

Figure 11 shows the result of the calculations in the form of two distributions of the positions of the cluster particles. The distributions with minimum and maximum potential energy values in the considered series of calculations are shown on the left and right. It can be clearly seen that the particles move away from the sphere as the potential energy increases. Note that the potential energy values are given in relative terms when it is assumed that the potential energy parameter $\varepsilon_N = 1$. Blue and black straight lines connecting the positions of the cluster particles are drawn for the convenience of depicting the cluster as a whole. The lengths of the blue and black edges are less than one and between one and two, respectively.

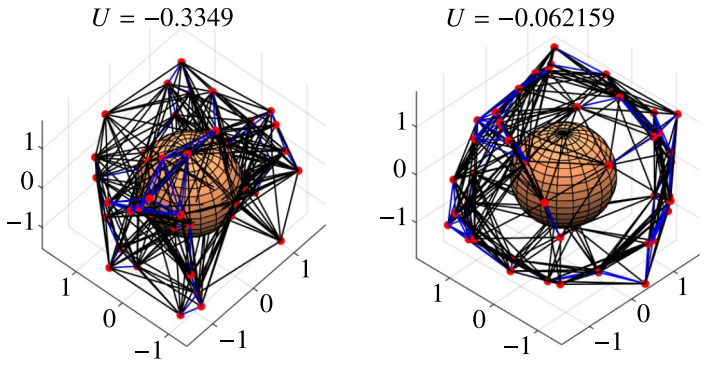

Figure 11. Mutual positioning of saddle and locally equilibrium configurations of cluster particles with $N = 50$

6. Examples of particle dynamics with a multiparticle potential

Let us consider the dynamics of cluster particles, taking into account the specifics of the multiparticle potential. Let at time t, $t \in [0, T]$ some locally equilibrium configuration $x_i(t)$, $y_i(t)$, $z_i(t)$, $i = 1, \ldots, N$ of the positions of the cluster particles be determined by solving the system of equations (14). In this case, the positions of the particles lie on the surface of a sphere of radius $q_{*,N}$, while the center of the sphere coincides with the center of symmetry of the cluster.

Consider the following scheme of random effects on the positions of cluster particles:

$$x_i \to x_i' = x_i + \rho\left(\xi_i - \frac{1}{N}\sum_{j=1}^{N}\xi_j\right) + N\Delta x,$$

$$y_i \to y_i' = y_i + \rho\left(\eta_i - \frac{1}{N}\sum_{j=1}^{N}\eta_j\right) + N\Delta y,$$

$$z_i \to z_i' = z_i + \rho\left(\zeta_i - \frac{1}{N}\sum_{j=1}^{N}\zeta_j\right) + N\Delta z,$$

where $i = 1, \ldots, N$, ρ — a small non-negative number, the amplitude of a random disturbance, ξ, η, ζ — uniformly random numbers from the segment [0, 1]; the vector $\Delta\mathbf{r} = (\Delta x, \Delta y, \Delta z)$ can be interpreted as the displacement vector of the cluster as a whole. We solve the system of equations (14) again, choosing as the initial particle distribution the values x_i', y_i', z_i', $i = 1, \ldots, N$. The found equilibrium positions of the particles $x_i(t+1)$, $y_i(t+1)$, $z_i(t+1)$, $i = 1, \ldots, N$ also lie on the surface of the sphere, they are considered as the next step in the dynamics of the cluster particles. Repeating the above procedure many times, we will construct the dynamics of the cluster particles.

Let the displacement vector of the cluster particles as a whole be absent at the beginning, i. e., $\Delta\mathbf{r} = \mathbf{0}$. In this case, it should be expected that the cluster particles will randomly wander along

the surface of the sphere, radius $q_{*,N}$. Figure 12 shows an example of calculating the dynamics of cluster particles when it was assumed that $N = 50$, $\rho = 0.05$, $T = 10^3$. As the initial distribution $x_i(0)$, $y_i(0)$, $z_i(0)$, $i = 1, \ldots, N$ the positioning of the cluster particles on a circle was chosen. In Figure 12, *a* and Figure 12, *b*, the initial positions of the cluster particles are marked with markers in the form of bold black dots. Figure 12, *a* shows the initial positioning of the cluster particles, as well as the further dynamics of three random particles from N. The trajectories of each of the three particles can be seen to randomly wander around the sphere. Figure 12, *b* shows the trajectories of all cluster particles.

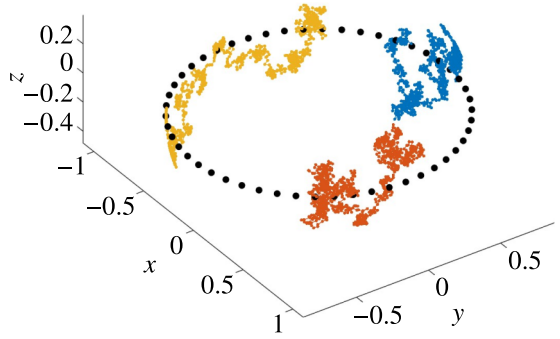

(a) Trajectories of three randomly selected cluster particles, $N = 50$

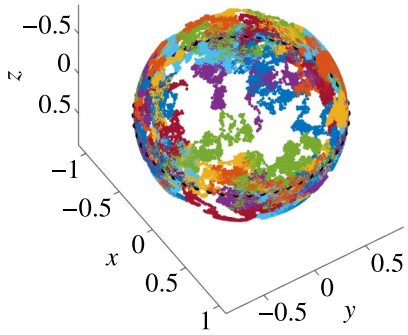

(b) Trajectories of all cluster particles, $N = 50$

Figure 12

The results of the computational experiment in Figure 12 demonstrate that the cluster particles, initially concentrated on a circle, tend to be quasi-uniformly distributed over the surface of the sphere, while the sphere as a whole is at rest.

Consider the motion of cluster particles for the case when the displacement vector $\Delta\mathbf{r}$ of the cluster as a whole is different from zero. To illustrate this case, we assume that the displacement depends on time and corresponds to a curve on the plane called the Bernoulli Lemniscate, which in appearance corresponds to the infinity symbol "∞". In this regard, let us assume that $\Delta\mathbf{r} = (LBx(t + 1) - LBx(t), LBy(t + 1) - LBy(t), 0)$, where a pair of functions $LBx(t)$, $LBy(t)$, defines a parametric entry of the Bernoulli Lemniscate, when $LBx(t) = \rho\frac{\cos\frac{2\pi t}{T}}{1+\sin^2\frac{2\pi t}{T}}$, $LBy(t) = \rho\frac{\sin\frac{2\pi t}{T}\cos\frac{2\pi t}{T}}{1+\sin^2\frac{2\pi t}{T}}$, $t \in [0, T]$.

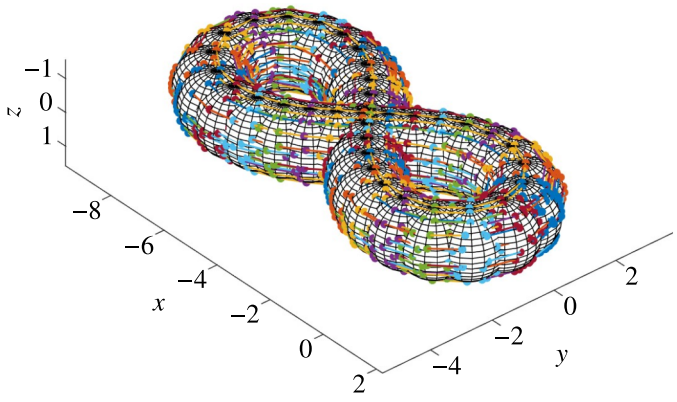

Figure 13. Movement of a cluster of particles along a curve close to the Bernoulli Lemniscate, $N = 100$

Figure 13 shows an example of a numerical implementation of cluster dynamics, provided that $N = 100$, $\rho = 0.05$, $T = 35$ and that the displacement of cluster particles followed the Bernoulli Lemniscate. The trajectories of the cluster particles are given for the convenience of perception, spheres

are constructed for each of the time points on which the positions of the equilibrium configurations of the cluster particles are located.

7. Marking the space using a combined potential

Let us consider the layout of the configuration space using a combination of binary U_2 and multiparticle potential U_N with maximum partiality. Taking into account (2), (4), (5) let us write down the desired potential:

$$U_{2,N} = \frac{\varepsilon'_2}{2} \sum_{i,\, j=1\ (i\neq j)}^{N} \phi(r_{i,j}) + \frac{\varepsilon'_N}{N} \sum_{i=1}^{N} \phi\left(\frac{q_i}{q_{*,N}}\right), \tag{15}$$

where $\phi(r) = \frac{m}{n-m} r^{-n} - \frac{n}{n-m} r^{-m}$, $q_i = |\mathbf{q}_i|$, $\mathbf{q}_i = \mathbf{r}_i - \mathbf{r}_{cs}$, $\mathbf{r}_{cs} = \frac{1}{N} \sum\limits_{j=1}^{N} \mathbf{r}_j$ — the center of symmetry of the cluster.

Within the framework of the combined potential (15), it is necessary to determine the choice of a pair of parameters ε'_2 and ε'_N. In section No. 3, devoted to the description of the cluster using a binary potential U_2, it was assumed that $\varepsilon'_2 = \varepsilon_2 = 1$. In section No. 5, where the multiparticle potential U_N was studied, it was assumed that $\varepsilon'_N = \varepsilon_N = 1$, at the same time, the potential value U_N for all equilibrium configurations was -1. If we assume that the interaction of particles in a cluster is described only by a multiparticle potential U_N, then it is necessary that the value of potential energy U_N in locally equilibrium configurations correspond to the characteristic values of potential energy, which we find after averaging the potential energies of locally equilibrium configurations with a binary potential.

Table 6. The average values of the potential energies of the equilibrium positions of the binary Mie potential ($n = 12$, $m = 6$) depending on the number of particles in the cluster N

N	2	3	4	5	6	7	8	12	15	20	25	30	50	100
$-\overline{U_2} \approx$	1	3	6	9	13	16	19	34	48	72	98	124	234	531

Thus, assuming that $U_N \cong \overline{U_2}$, where $\overline{U_2}$ is the average value of the potential energies of locally equilibrium configurations of the binary potential of Mi, we find $\varepsilon_N = -\overline{U_2}$. Table 6 shows the values of the average potential values of the locally equilibrium positions of the binary potential, depending on the number of particles in the cluster.

According to Table 6, a suitable regression curve $\varepsilon_N = 2.663N + 0.170 \cdot N^{1.6}$, $N \geqslant 2$ was constructed, whose the coefficients are highly significant at a level not less than the value $6.8 \cdot 10^{-8}$.

As a result, it turns out that the cluster can be described both in terms of binary and multiparticle potentials. After taking into account the dependence $\varepsilon_N = 2.663N + 0.170 \cdot N^{1.6}$ on N both potentials U_2 and U_N become comparable and can be mutually combined, e. g., according to the additive scheme, when it is assumed that

$$\varepsilon'_2 = \varepsilon_2(1-\sigma) = 1 - \sigma, \quad \varepsilon'_N = \sigma\varepsilon_N = \sigma\left(2.663N + 0.170 \cdot N^{1.6}\right), \tag{16}$$

where $\sigma \in [0, 1]$ — a parameter describing the proportion of the multiparticle potential in the cluster description.

Let us define the procedure for searching for locally equilibrium configurations of cluster particles with potential energy (15) according to scheme (16) by the gradient descent method, i. e.

$$\begin{aligned}
\dot{x}_i &= -\frac{\partial U_{2,N}}{\partial x_i} = -\varepsilon_2' \sum_{k\neq i} \mu(r_{i,k}) x_{i,k} - \frac{\varepsilon_N'}{N q_{*,N}^2}\left[\mu\left(\frac{q_i}{q_{*,N}}\right)(x_i - x_{cs}) - \frac{1}{N}\sum_{k=1}^{N}\mu\left(\frac{q_k}{q_{*,N}}\right)(x_k - x_{cs})\right],\\
\dot{y}_i &= -\frac{\partial U_{2,N}}{\partial y_i} = -\varepsilon_2' \sum_{k\neq i} \mu(r_{i,k}) y_{i,k} - \frac{\varepsilon_N'}{N q_{*,N}^2}\left[\mu\left(\frac{q_i}{q_{*,N}}\right)(y_i - y_{cs}) - \frac{1}{N}\sum_{k=1}^{N}\mu\left(\frac{q_k}{q_{*,N}}\right)(y_k - y_{cs})\right],\\
\dot{z}_i &= -\frac{\partial U_{2,N}}{\partial z_i} = -\varepsilon_2' \sum_{k\neq i} \mu(r_{i,k}) z_{i,k} - \frac{\varepsilon_N'}{N q_{*,N}^2}\left[\mu\left(\frac{q_i}{q_{*,N}}\right)(z_i - z_{cs}) - \frac{1}{N}\sum_{k=1}^{N}\mu\left(\frac{q_k}{q_{*,N}}\right)(z_k - z_{cs})\right],
\end{aligned} \tag{17}$$

where $\mu(r) = \frac{\phi'(r)}{r} = \frac{nm}{n-m}\left(-r^{-n-2} + r^{-m-2}\right)$. In the calculation results presented below, it was assumed that $n = 12$, $m = 6$.

Table 7 shows the results of a computational experiment to calculate the number of locally equilibrium configurations N_{lm} in a cluster consisting of $N = 12$ particles. In each of their experiments $M = 3 \cdot 10^5$ calculations of the system of equations (17) with random initial positions of the cluster particles were performed. It was also assumed that $L = -\frac{1}{2} + \frac{1}{4}\sqrt[3]{\frac{4}{3}\pi N}$, $\delta = 10^{-10}$, $\delta_c = 0.05$.

Table 7. Dependence of the number of equilibrium configurations on the proportion of the multiparticle potential, $N = 12$

σ	0	0.01	0.25	0.5	0.75	$1 - 10^{-2}$	$1 - 10^{-4}$	1
N_{lm}	358	285	156	93	42	5	1	∞

According to the results of the computational experiment presented in Table 7, by varying the proportion σ of the multiparticle contribution to potential energy, it is possible to vary the number of equilibrium configurations in the cluster up to the construction of a single configuration. The implementation of a single equilibrium configuration means that over time, with arbitrary shaking of the positions of particles in the cluster, they occupy well-defined positions, while the equilibrium configuration as a whole is invariant with respect to shifts and rotation of the cluster as a whole.

Figure 14 shows the results of calculating a cluster with the number of particles $N = 50$ in two cases when $\sigma = 1 - 10^{-6}$ and $\sigma = 1$. It is clear that the spherical shape of the cluster is provided by the main contribution to the potential of the multiparticle component. In Figure 14, *a*, a more or less uniform arrangement of particles on the sphere is ensured by a binary contribution to the potential. In Figure 14, *b*, the random distribution of particles on the sphere is, determined by the initial random positioning of particles when solving the problem (17). A graph of one of an infinite number of possible locally equilibrium configurations is given. The lines highlight those segments whose length does not exceed 0.85.

The study of the dependence of the number of saddle configurations on the parameter σ was carried out using the example of several clusters with $N = 3, 4, 5$. The problem (11), (12) with a combined potential energy (15) has been repeatedly solved, provided that $L = \frac{1}{4}\sqrt[3]{\frac{4}{3}\pi N}$. For a cluster with $N = 3$, the number of saddle configurations turned out to be several units, when $\sigma \in [0, 1]$, at the same time, it was assumed that $\delta = 10^{-10}$, $\delta_c = 0.05$. For clusters with $N = 4, 5$ the number of saddle configurations was finite at $\sigma \in [0, 1)$, $\delta = 10^{-10}$, $\delta_c = 0.05$. The number of saddle configurations became infinite at $\sigma = 1$, it was assumed that $\delta = 10^{-4}$. Apparently, the same pattern will remain for all other clusters with $N > 5$ as for clusters with $N = 4, 5$, i. e., at $\sigma \in [0, 1)$ the number of saddle configurations will be finite, while for $\sigma = 1$ — the number will be infinite.

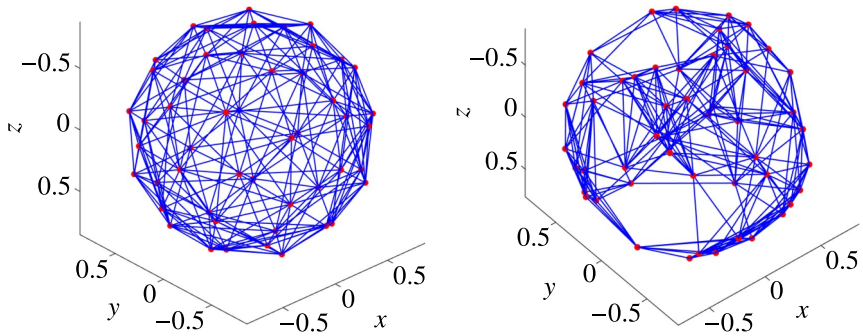

(a) A single equilibrium configuration in the case when $N = 50$, $\sigma = 1 - 10^{-6}$

(b) One of the possible locally equilibrium configurations in the case when $N = 50$, $\sigma = 1$

Figure 14

8. Conclusion

The paper presents a formulation and some approaches to the problem of choosing a solution in the classical format of describing a molecular system. The classical format of description in terms of molecular dynamics and the potential energy function provides an understandable way to choose a particular solution or, stated otherwise, a way to mark up the configuration space with a set of stationary points of the potential energy function. The marking of the configuration space using the potential energy function can be used in the problem of choosing a solution in the quantum mechanical format of describing a molecular system, for example, in connection with the theory of quantum measurement.

The choice of one or another markup of the configuration space is related to the following two physical and mathematical problems. A direct selection problem arises when the potential energy function is given and a set of stationary points is obtained from it. Conversely, the inverse choice problem occurs when a set of stationary points is given and it is necessary to reconstruct the corresponding potential energy function from it. The present work considers the direct problem of choice.

The potential energy function of a monatomic molecular system from a set of multiparticle contributions has been constructed along with an algorithm defined for constructing a spectrum of multiparticle potentials. The features of the configuration space markup using a binary potential and a multiparticle potential of maximum partiality are considered in detail. If the number of stationary points is large but finite at a binary potential, the set of stationary points can be infinite at a multiparticle potential under certain conditions. When combining binary and multiparticle potentials, the possibility of influencing the markup of the configuration space by changing the number and location of stationary points is demonstrated.

References

Биритейн Т. М., Птицын О. Б. Конформации макромолекул. — М.: Наука, 1964. — 391 с.
Birshtejn T. M., Pticyn O. B. Konformacii makromolekul [Conformations of macromolecules]. — Moscow: Nauka, 1964. — 391 p. (in Russian).

Броер Х.-П., Петруччионе Ф. Теория открытых квантовых систем. — Ижевск: НИЦ «Регулярная и хаотическая динамика», 2010. — 800 с.
Breuer H.-P., Petruccione F. The theory of open quantum systems. — New York: Oxford University, 2002. — 636 p. (Russ. ed.: *Broer Kh.-P., Petruchchione F.* Teoriya otkrytykh kvantovykh sistem. — Izhevsk: NITs “Regulyarnaya i khaoticheskaya dinamika”, 2010. — 800 p.)

Менский М. Б. Группа путей измерения. Поля. Частицы. — М.: Наука, 1983. — 319 с.
Menskij M. B. Gruppa putej izmereniya. Polya. Chasticy [Group of measurement paths. Fields. Particles]. — Moscow: Nauka, 1983. — 319 p. (in Russian).

Плохотников К. Э. О статистическом генераторе решений уравнения Шрёдингера // Математическое моделирование. — 2022a. — Т. 34, № 12. — С. 75–90.
Plokhotnikov K. E. On the statistical generator of solutions to the Schrödinger equation // Mathematical Models and Computer Simulations. — 2023. — Vol. 15, No. 4. — P. 591–600. (Original Russian paper: *Plokhotnikov K. E.* O statisticheskom generatore reshenii uravneniya Shredingera // Matematicheskoe modelirovanie. — 2022a. — Vol. 34, No. 12. — P. 75–90.)

Плохотников К. Э. Об одном методе численного решения уравнения Шрёдингера // Математическое моделирование. — 2019. — Т. 31, № 8. — С. 61–78.
Plokhotnikov K. E. About one method of numerical solution of Schrödinger's equation // Mathematical Models and Computer Simulations. — 2020. — Vol. 12, No. 2. — P. 221–231. (Original Russian paper: *Plokhotnikov K. E.* Ob odnom metode chislennogo resheniya uravneniya Shredingera // Matematicheskoe modelirovanie. — 2019. — Vol. 31, No. 8. — P. 61–78.)

Плохотников К. Э. Об одном численном методе нахождения позиций ядер водорода и кислорода в кластере воды // Математическое моделирование. — 2022b. — Т. 34, № 4. — С. 43–58.
Plokhotnikov K. E. About one numerical method for finding the positions of hydrogen and oxygen nuclei in a water cluster // Mathematical Models and Computer Simulations. — 2022. — Vol. 14, No. 6. — P. 900–909. (Original Russian paper: *Plokhotnikov K. E.* Ob odnom chislennom metode nakhozhdeniya pozitsii yader vodoroda i kisloroda v klastere vody // Matematicheskoe modelirovanie. — 2022b. — Vol. 34, No. 4. — P. 43–58.)

Плохотников К. Э. Численный метод реконструкции средних позиций квантовых частиц в молекулярной системе // Математическое моделирование. — 2020. — Т. 32, № 9. — С. 20–34.
Plokhotnikov K. E. Numerical method for reconstructing the average positions of quantum particles in a molecular system // Mathematical Models and Computer Simulations. — 2021. — Vol. 13, No. 3. — P. 372–381. (Original Russian paper: *Plokhotnikov K. E.* Chislennyi metod rekonstruktsii srednikh pozitsii kvantovykh chastits v molekulyarnoi sisteme // Matematicheskoe modelirovanie. — 2020. — Vol. 32, No. 9. — P. 20–34.)

Товбин Ю. К. Метод молекулярной динамики в физической химии. — М.: Наука, 1996. — 334 с.
Tovbin Yu. K. Metod molekulyarnoj dinamiki v fizicheskoj ximii [The method of molecular dynamics in physical chemistry]. — Moscow: Nauka, 1996. — 334 p. (in Russian).

Хартри Д. Расчеты атомных структур / под ред. В. А. Фока. — М.: Изд-во иностр. лит., 1960. — 271 с.
Hartree D. R. The calculation of atomic structures. — New York: Wiley, 1957. — 181 p. (Russ. ed.: *Khartri D.* Raschety atomnykh struktur / pod red. V. A. Foka. — Moscow: Izd-vo inostr. lit., 1960. — 271 p.)

Amber Project. — [Электронный ресурс]. — https://ambermd.org/contributors.html (accessed: 19.07.2023).

Car R., Parrinello M. Unified approach for molecular dynamics and density-functional theory // Physical Review Letters. — 1985. — Vol. 55, No. 22. — P. 2471–2474.

Chakraborty D., Banerjee A., Wales D. J. Side-chain polarity modulates the intrinsic conformational landscape of model dipeptides // J. Phys. Chem. B. — 2021. — Vol. 125. — P. 5809–5822.

Frenkel D., Smit B. Understanding molecular simulation. From algorithms to applications. — New York: Academic Press, 2002. — 658 p.

Hirschfelder J. O., Curtiss C. F., Bird R. B. Molecular theory of gases and liquids. — New York: Wiley, 1954. — 1219 p.

HyperChem 8.0. — [Электронный ресурс]. — https://hyperchem.software.informer.com (accessed: 19.07.2023).

Kim J., Baczewski A. T., Beaudet T. D. et al. QMCPACK: an open source ab initio quantum Monte Carlo package for the electronic structure of atoms, molecules and solids // Journal of Physics Condensed Matter. — 2018. — Vol. 30, No. 19.

Kohn W. Nobel Lecture: Electronic structure of matter — wave functions and density functionals // Reviews of Modern Physics. — 1999. — Vol. 71, No. 5. — P. 1253–1266.

Kühne T. D., Iannuzzi M., Del Ben M. et al. DCP2K: An electronic structure and molecular dynamics software package -Quickstep: Efficient and accurate electronic structure calculations // J. Chem. Phys. — 2020. — Vol. 152, No. 194103. — P. 1–48.

Marx D., Hutter J. Ab initio molecular dynamics: basic theory and advanced methods. — New York: Cambridge University Press, 2009. — 580 p.

Plokhotnikov K. E. Modeling of water clusters by numerical solution of the Schrödinger equation // Physics of Wave Phenomena. — 2022. — Vol. 30, No. 3. — P. 156–168.

Plokhotnikov K. E. On the set of solutions to the Schrödinger equation as illustrated with the description of water clusters // Physics of Wave Phenomena. — 2023. — Vol. 31, No. 3. — P. 151–159.

Plokhotnikov K. E. Solving the Schrödinger equation on the basis of finite-difference and Monte Carlo approaches // Journal of Applied Mathematics and Physics. — 2021. — Vol. 9, No. 2. — P. 328–369.

Röder K., Wales D. J. The energy landscape perspective // Frontiers in Molecular Biosciences. — 2022. — Vol. 9, No. 820792. — P. 1–9.

Schlosshauer M. The quantum-to-classical transition and decoherence // https://doi.org/10.48550/arXiv.1404.2635

Stillinger F. H., LaViolette R. A. Local order in quenched states of simple atomic substances // Phys. Rev. B. — 1986. — Vol. 34, No. 9. — P. 5136–5144.

Stillinger F. H., Weber T. A. Packing structures and transitions in liquids and solids // Science. — 1984. — Vol. 225, No. 4666. — P. 983–989.

Wales D. J. Calculating rate constants and committor probabilities for transition networks by graph transformation // J. Chem. Phys. — 2009. — Vol. 130, No. 204111. — P. 1–7.

Wales D. J. Discrete path sampling // Molecular Physics. — 2002. — Vol. 100, No. 2. — P. 3285–3305.

Zurek W.H. Quantum theory of the classical: einselection, envariance, quantum darwinism and extantons // Entropy. — 2022. — Vol. 24, No. 1520. — P. 1–100.